killed at 7 weeks after colitis induction, and the severity of colitis was examined using the disease activity parameters BW and histological score. The expression levels of macrophage inflammatory protein (MIP)-2 and IL-1β in intestinal tissues were determined using real-time polymerase chain reaction (PCR).

Enzyme-linked Immunosorbent Assay

Concentrations of murine IL-10 were measured in cell culture supernatants using a specific enzyme-linked immunosorbent assay kit, according to the manufacturer's instructions.

Histological Examinations

Tissues taken from the distal part of the colon were formalin-fixed and embedded in paraffin blocks. For histological examinations, 3-μm paraffin sections were stained with hematoxylin and eosin to visualize their general morphology under a light microscope. Histological grading was evaluated as previously described.[24]

RNA Extraction and Real-time PCR

Total RNA was extracted from each sample using an RNeasy Protect Mini Kit (Qiagen Inc., Tokyo, Japan), then equal amounts of RNA were reverse transcribed into complementary DNA using a QPCR cDNA Kit (Stratagene, La Jolla, CA). All primers (see Table, Supplemental Digital Content 1, http://links.lww.com/IBD/A629, for the primer sequences) used were flanked by intron–exon junctions using the National Center for Biotechnology Information blast tool and Primer3 software. Quantitative real-time PCR was performed using a StepOnePlus Real-Time PCR System (Applied Biosystems, Foster City, CA) with SYBR Green PCR master mix (Applied Biosystems), according to the manufacturer's instructions. The levels of messenger RNA were normalized to that of β-actin using sequence detector software (Applied Biosystems).

Antigen-induced Arthritis in Rabbits

Arthritis was induced by injection of ovalbumin (OVA; Sigma–Aldrich, St Louis, MO) into joints of OVA-immunized rabbits according to the method of Pettipher et al.[25] Briefly, Japanese white rabbits (kb1) weighing approximately 3 kg (Kitayama LABES, Nagano, Japan) were immunized by intradermal injection of 4 mg OVA in 1 mL of Freund's complete adjuvant (Gibco, Paisley, Scotland). The animals were reimmunized 14 days later in the same manner. Five days after the second immunization, arthritis was induced in a knee joint by intra-articular injection of 5 mg OVA in 1 mL of sterile saline, whereas the contralateral knee joint was injected with 1 mL sterile saline to serve as a within animal control.

GMA for Rabbit Arthritis Model

GMA for rabbit arthritis model was established as reported by Kashiwagi et al.[26] We used a mini GMA column with a diameter of 1.5 cm and length of 10 cm, which contained 11 g of cellulose diacetate carriers (G-1 beads) developed by JIMRO Co. Ltd. (Takasaki, Japan) for the Adacolumn. The G-1 beads have a diameter of approximately 2 mm. Apheresis was performed at a flow rate of 1.5 mL/min for 60 minutes. Small size columns with a volume equal to the priming volume of the GMA column but without carriers were used as sham columns (Fig. 5A). It has been shown that immunoglobulin and complement fragments such as C3bi deposit onto G-1 beads during apheresis, and then granulocytes and monocytes are selectively adsorbed to the beads by using their Fc receptor and complement receptor.[27]

Detection of Superoxide Generation by Leukocytes in GMA Column

Superoxide generation in the GMA column was detected according to the method of Nakano et al.[28] Briefly, each rabbit was continuously infused with 185 μM of a lucigenin derivative of Cypridinacea (2-methyl-6-[p-methoxyphenyl]-3,7-dihydroimidazo-[1,2-a]pyrazin-3-one [MCLA]) at a flow rate of 10 mL/h starting 10 minutes before initiation of GMA. The GMA column was placed inside the chamber of a photon counting unit shielded from light, and then GMA was performed. The amount of O_2^- (superoxide anion radical) was measured by directly counting the photons emitted by MCLA on reaction with O_2^-.

Measurement of Apoptotic Neutrophils from Rabbit Peripheral Blood

Blood was collected using acid citrate dextrose as an anticoagulant to minimize neutrophil activation and maintain stability. Neutrophils were isolated using discontinuous Percoll gradients (Pharmacia Fine Chemicals, Piscataway, NJ) (65% and 70% in diluted PBS) by slight modification of a method previously described.[29] Isolated neutrophils at 1×10^6 cells per milliliter in RPMI 1640 medium supplemented with 10% fetal bovine serum were incubated at 37°C in a CO_2 incubator for 18 hours. Apoptosis of neutrophils was assessed using a previously published procedure.[30] Briefly, cultured neutrophils at 1×10^6 cells per milliliter were washed with PBS and fixed for 30 minutes in ice-cold 70% ethanol. Fixed cells were then washed twice with cold PBS and resuspended in 500 μL of PBS containing 250 μg/mL RNase and 5 μg/mL of propidium iodide. The suspension was incubated in the dark at room temperature for 15 minutes before analysis with an FACScan (BD Bioscience). The proportion of cells within the hypodiploid peak has been shown to correlate with apoptosis.[30]

Peritoneal Exudate Cells Isolation and Apoptosis Induction by Hydrogen Peroxide

Peritoneal exudate cells (PECs), containing 65% to 85% neutrophils,[31] were isolated using a previously described method with minor modifications.[31,32] Mice were injected intraperitoneally with 1 mL of 2% sodium caseinate (Wako Pure Chemical Industries, Osaka, Japan) in PBS. Twenty hours later, PECs were collected by lavage of the peritoneum of each mouse with Hank's Balanced Salt Solution in a total volume of 8 mL containing 1 U/mL heparin. The PECs were then incubated at a concentration of 2×10^6 cells per milliliter in RPMI 1640 medium supplemented with 100 U/mL penicillin (Invitrogen), 100 μg/mL

streptomycin (Invitrogen), and 500 μM H_2O_2 (Sigma–Aldrich) for 1 hour at 37°C with 5% CO_2. AC death stage was analyzed using a PE Annexin V apoptosis detection kit I (BD Biosciences Pharmingen) with a FACSCalibur (BD Biosciences Pharmingen). After extensive washing, these apoptotic PECs (APECs) were injected intravenously for in vivo experiments.

Flow Cytometric Analysis of L-selectin Expression on Neutrophils

Rabbit Model

First, 200 μL of an EDTA-blood sample was labeled with FITC-conjugated anti–L-selectin monoclonal antibody (LAM1-3; Beckman Coulter, Hialeah, FL) for 30 minutes at 4°C, and then incubated blood cells were treated with 2 mL of FACS lysing solution (Becton Dickinson, San Jose, CA) for 10 minutes at room temperature. After washing twice with PBS containing 0.1% NaN_3, 500 μL of 1% paraformaldehyde in PBS was added and subjected to flow cytometry. Neutrophils were discerned by a combination of low-angle forward-scattered and right-angle–scattered laser light, and more than 5000 events were acquired in the gate.

Mouse Model

First, 5×10^5 of live or APECs from an AKR mouse were labeled with PE-conjugated anti-CD62L monoclonal antibody (Beckman Coulter) for 30 minutes at 4°C. After washing twice with PBS, 500 μL of PBS was added, and the samples were subjected to flow cytometry.

Statistical Analysis

All results are expressed as the mean with the SEM or as a range, as appropriate. Student's *t* test, Mann–Whitney U test, and Wilcoxon signed-rank test were used as appropriate to examine significant differences. *P*-values less than 0.05 were considered significant. All statistical analyses were performed using statistical analysis software (SPSS, version 12.0 for the PC; SPSS Japan Inc., Tokyo, Japan).

RESULTS

ACs Do Not Ameliorate Chronic Colitis in SCID Mice in Absence of Mature B Cells

Adoptive transfer of $CD4^+$ T cells isolated from the MLNs of SAMP1 mice induced remarkable intestinal inflammation in mature B- and T-cell–negative SCID mice.[22] To investigate the effects of ACs on intestinal inflammation, we used an SAMP1 $CD4^+$ MLN T-cell–induced chronic colitis model of SCID mice. Dexamethasone (Dex)-induced apoptotic thymocytes (Fig. 1B) or the vehicle (PBS) was injected intravenously into the chronic colitis model after transfer of $CD4^+$ MLN T cells from SAMP1 mice (Fig. 1A), and then changes in several inflammatory parameters were evaluated. The inflammatory parameters BW loss (Fig. 1C), colon shortening (Fig. 1D, E), and histological scores for the large intestine (Fig. 1F, G) showed similar levels of severity in the chronic colitis mice after transfer of ACs or PBS. In addition, the expression levels of proinflammatory cytokines, IL-1β, and MIP-2 were similar between the AC and PBS groups (Fig. 1H).

ACs Adoptively Cotransferred with $CD19^+$ B Cells Ameliorate Intestinal Inflammation in Chronic Colitis Mice

We next investigated the effects of ACs in the presence of cotransferred $CD19^+$ splenocytes on chronic intestinal inflammation. ACs or the vehicle (PBS) was injected intravenously into the chronic colitis model after transfer of $CD19^+$ splenocytes from AKR mice and $CD4^+$ MLN T cells from SAMP1 mice (Fig. 2A), and then changes in several inflammatory parameters in both groups were evaluated. The inflammatory parameters BW loss (Fig. 2B), colon shortening (Fig. 2C, D), and histological scores for the large intestine in chronic colitis mice were significantly less severe in the AC group as compared with those in the PBS group (Fig. 2E, F). In addition, the expression levels of IL-1β and MIP-2 were also significantly lower in the AC group (Fig. 2G).

Cotransfer with CD19hiCD1dhi-depleted B Cells Tends to Deteriorate Intestinal Inflammation

We further investigated whether the effects of ACs on chronic intestinal inflammation are dependent on the subpopulation of regulatory B cells. Recently, we reported that CD19hiCD1dhi B cells produce high levels of IL-10 and were considered to be a Bregs population.[22] Consequently, a CD19hiCD1dhi-depleted B-cell population can be considered to be a Breg-depleted B–cell population. ACs or the vehicle (PBS) was injected intravenously into the chronic colitis model after transfer of CD19hiCD1dhi-depleted B cells from AKR mice and $CD4^+$ MLN T cells from SAMP1 mice (Fig 3A, B), and then changes in several inflammatory parameters in both groups were evaluated. The inflammatory parameters BW loss (Fig. 3C), colon shortening (Fig. 3D, E), and histological scores for the large intestine (Fig. 3F, G) in the chronic colitis mice were slightly more severe in the AC group as compared with those in PBS group, although the difference was not significant. Also, the expression levels of IL-1β and MIP-2 were slightly higher in the AC group, although again the difference was not significant (Fig. 3H).

ACs Induce IL-10 Production in Splenic B Cells

To investigate possible interaction between ACs and B cells, we injected Dex-induced syngeneic apoptotic thymocytes (Fig. 1B) or the vehicle alone (PBS) into AKR mice. Three weeks later, $CD19^+$ splenocytes from both groups were cultured in the presence or absence of PMA and ionomycin. IL-10–producing B cells were found in the AC group at increased frequency as compared with the PBS group under both stimulated and unstimulated conditions (Fig. 4A). Furthermore, B cells from the AC group produced a significantly higher level of IL-10 as compared with those from the PBS group under both conditions (Fig. 4B).

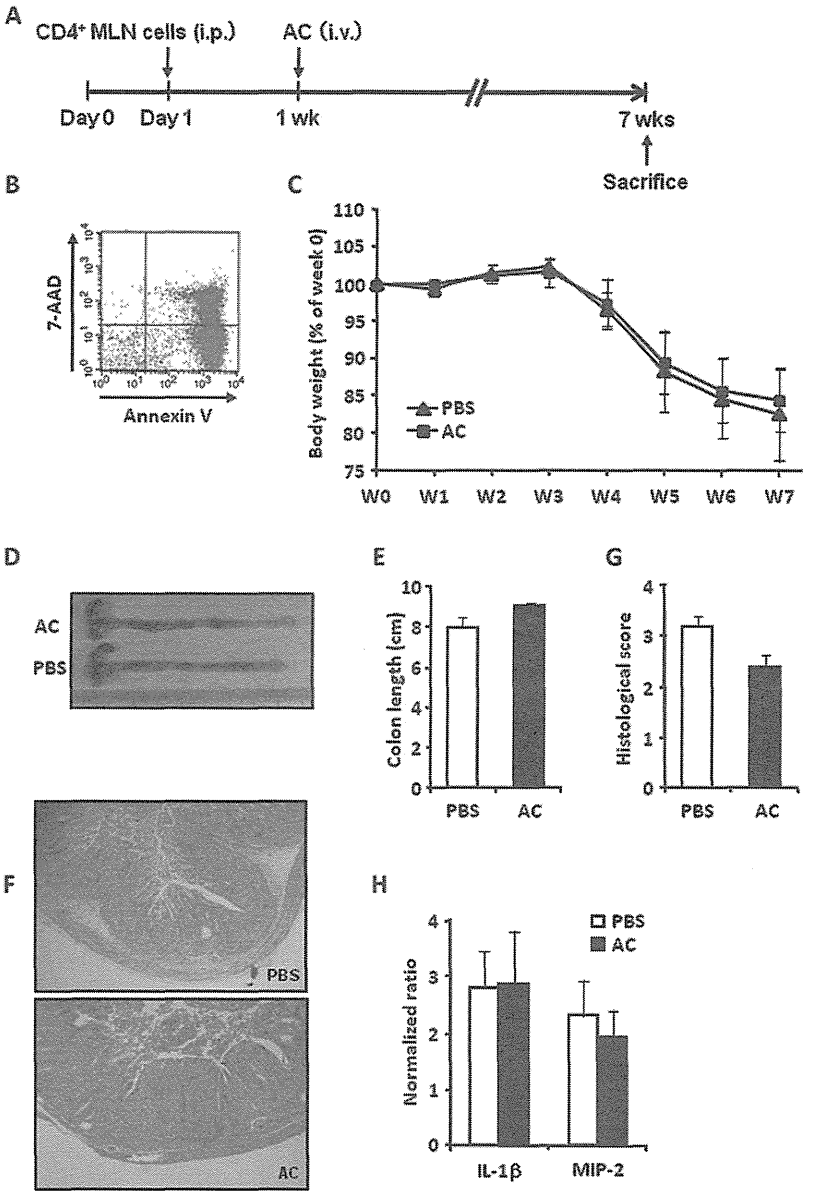

FIGURE 1. ACs alone did not ameliorate intestinal inflammation in SAMP1 CD4+ MLN T-cell–induced chronic colitis mice. A, Protocol for induction of SAMP1 CD4+ MLN T-cell–mediated chronic colitis in SCID mice and AC injection. Purified CD4+ T cells (5×10^5 cells per mouse) derived from MLN cells of SAMP1 mice were injected intraperitoneally on day 1 into 8- to 10-week-old SCID mice. B, Dex-treated thymocytes were subjected to flow cytometry after staining with annexin V and 7-AAD. C, Effects of ACs on BW changes in SAMP1 CD4+ MLN Tcell–induced chronic colitis. The AC group (squares) was given an intravenous injection of ACs (1×10^7 cells per mouse) on week 1, whereas the control group received the vehicle alone (triangle). Data are expressed as serial changes in percentage of weight change over a 7-week period. Error bars indicate SEM values obtained from mice in each group (n = 5). D, Representative images of colons dissected from mice in each experimental group. E, Effects of ACs on colon length in SAMP1 CD4+ MLN T-cell–induced chronic colitis. Error bars indicate SEM values obtained from mice in each group (n = 5). F, Representative images of histological changes in large intestines at 7 weeks after SAMP1 CD4+ MLN T-cell injection with or without ACs. G, Mean values of intestinal histological scores in each experimental group. Error bars indicate SEM values obtained from mice in each group (n = 5). H, Gene expressions of IL-1β and MIP-2 in large intestines in each experimental group. Error bars indicate SEM values obtained from mice in each group (n = 5).

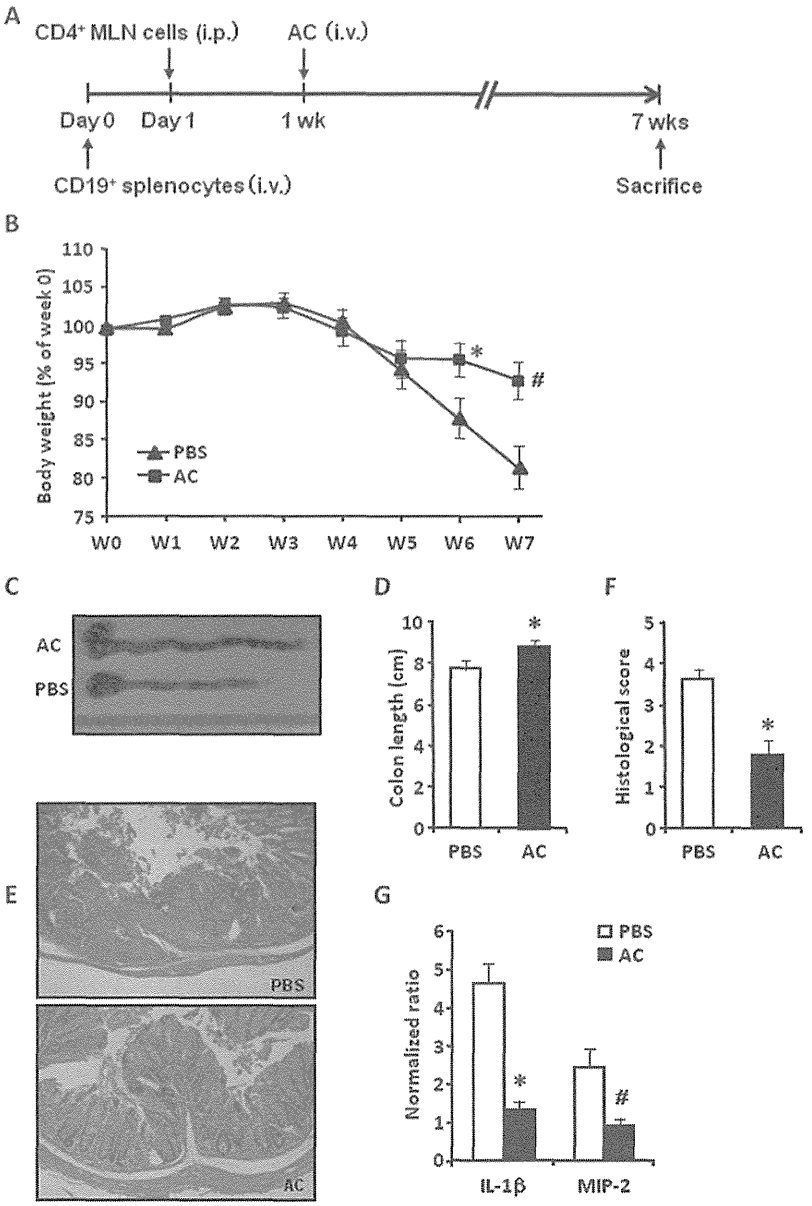

FIGURE 2. ACs ameliorated intestinal inflammation in SAMP1 CD4+ MLN T-cell–induced chronic colitis mice when cotransferred with CD19+ splenocytes. A, Protocol for cotransfer of CD19+ splenocytes and ACs in SAMP1 CD4+ MLN T-cell–induced chronic colitic SCID mice. Purified whole CD19+ splenocytes (2×10^6 cells per mouse) derived from AKR mice and SAMP1 CD4+ MLN T cells (5×10^5 cells per mouse) were injected intravenously on day 0 and intraperitoneally on day 1, respectively, into 8- to 10-week-old SCID mice. B, Effects of ACs on BW changes in CD19+ splenocytes injected into SAMP1 CD4+ MLN T-cell–induced chronic colitic mice. The AC group (squares) was given an intravenous injection of ACs (1×10^7 cells per mouse) on week 1, whereas the control group received the vehicle alone (triangle). Data are expressed as serial changes in percentage of weight change over a 7-week period. Error bars indicate SEM values obtained from mice in each group (n = 9) (*$P < 0.04$ and #$P < 0.01$ versus PBS). C, Representative images of colons dissected from mice in each experimental group. D, Effects of ACs on colon length in CD19+ splenocytes injected into SAMP1 CD4+ MLN T-cell–induced chronic colitic mice. Error bars indicate SEM values obtained from mice in each group (n = 9) (*$P < 0.02$ versus PBS). E, Representative images of histological changes in large intestines at 7 weeks after injection of CD19+ splenocytes and SAMP1 CD4+ MLN T cells with or without ACs. F, Mean values of intestinal histological scores in each experimental group. Error bars indicate SEM values obtained from mice in each group (n = 9) (*$P < 0.01$ versus PBS). G, Gene expressions of IL-1β and MIP-2 in large intestines in each experimental group. Error bars indicate SEM values obtained from mice in each group (n = 9) (*$P < 0.001$ and #$P < 0.02$ versus PBS).

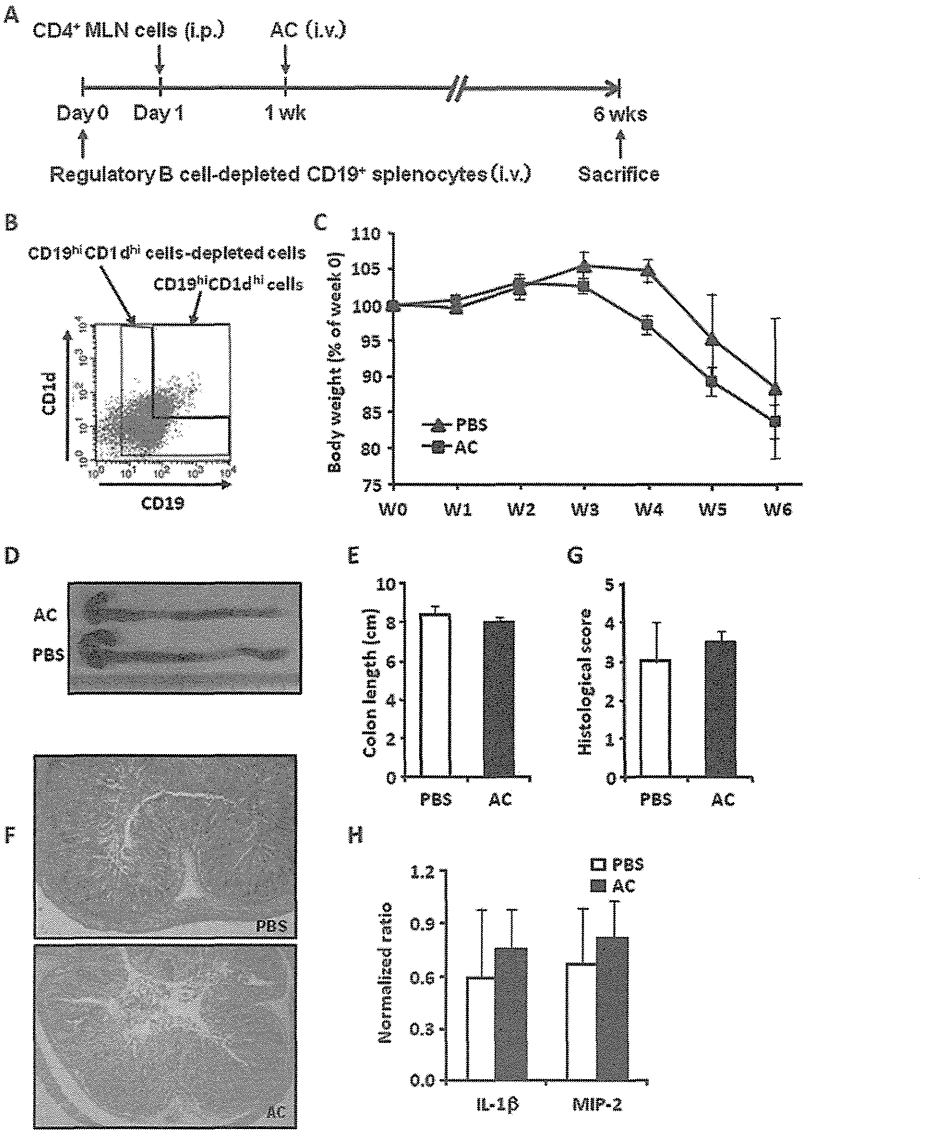

FIGURE 3. AC-mediated ameliorative effects were lost in the absence of the subpopulation of Bregs. A, Protocol for cotransfer of Bregs-depleted CD19+ splenocytes and ACs in SAMP1 CD4+ MLN T-cell–induced chronic colitic SCID mice. Flow cytometry-sorted CD19hiCD1dhi-depleted B cells (2×10^6 cells per mouse) derived from AKR mice and SAMP1 CD4+ MLN T cells (5×10^5 cells per mouse) were injected intravenously on day 0 and intraperitoneally on day 1, respectively, into 8- to 10-week-old SCID mice. B, CD19hiCD1dhi-depleted B cells were sorted by flow cytometry from CD19+ splenocytes derived from 15- to 25-week-old AKR mice. C, Effects of ACs on BW changes after injection of CD19hiCD1dhi-depleted B cells into SAMP1 CD4+ MLN T-cell–induced chronic colitic mice. The AC group (squares) was given an intravenous injection of ACs (1×10^7 cells per mouse) on week 1, whereas the control group received the vehicle alone (triangle). Data are expressed as serial changes in percentage of weight change over a 6-week period. Error bars indicate SEM values obtained from mice in each group (n = 4). D, Representative images of colons dissected from mice in each experimental group. E, Effects of ACs on colon length after injection of CD19hiCD1dhi-depleted B cells into SAMP1 CD4+ MLN T-cell–induced chronic colitic mice. Error bars indicate SEM values obtained from mice in each group (n = 4). F, Representative images of histological changes in large intestines at 6 weeks after injection of CD19hiCD1dhi-depleted B cells and SAMP1 CD4+ MLN T cells with or without ACs. G, Mean values of intestinal histological scores in each experimental group. Error bars indicate SEM values obtained from mice in each group (n = 4). H, Gene expressions of IL-1β and MIP-2 in large intestines in each experimental group. Error bars indicate SEM values obtained from mice in each group (n = 4).

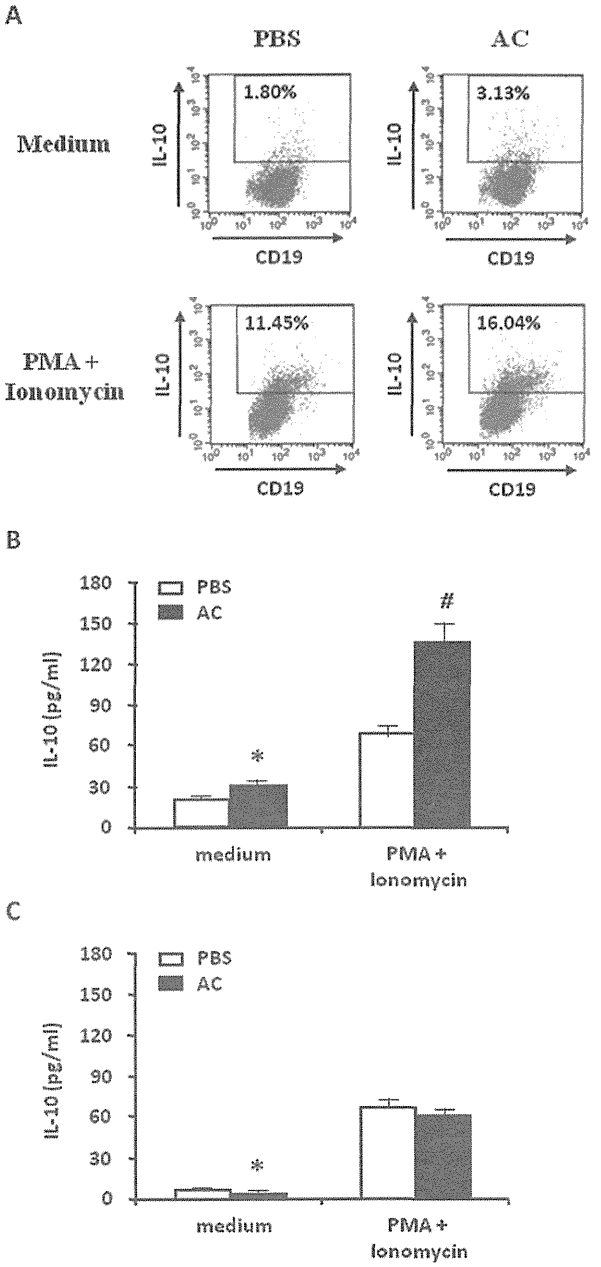

FIGURE 4. ACs induced IL-10 production in splenic B cells only in the presence of normal phagocytic function. A, Effects of AC injection on the number of splenic B cells expressing IL-10 in AKR mice. The AC group was given an intravenous injection of syngeneic ACs (1×10^7 cells per mouse), whereas the control group received the vehicle (PBS) alone. Three weeks later, CD19$^+$ splenocytes were harvested from both groups and cultured for 72 hours in the presence or absence of PMA and ionomycin. The expressions of CD19 and IL-10 were examined by flow cytometry. Representative dot plots showing expressions of CD19 and IL-10 in B cells are presented. B, Effects of AC injection on production of IL-10 by splenic B cells in AKR mice. The AC group (blocked column) were given an intravenous injection of syngeneic ACs (1×10^7 cells per mouse), whereas the control group received the vehicle (PBS) alone (open column). Three weeks later, CD19$^+$ splenocytes were harvested from both groups and cultured for 72 hours in the presence or absence of PMA and ionomycin, and then supernatants were collected and IL-10 production was measured by ELISA. Error bars indicate SEM values obtained from mice in each group (n = 3) (*$P < 0.001$ and #$P < 0.002$ versus PBS). C, Effects of AC injection on production of IL-10 by splenic B cells in MFG-E8 KO mice. The AC group (blocked column) was given an intravenous injection of syngeneic ACs (1×10^7 cells per mouse), whereas the control group received the vehicle (PBS) alone (open column). Three weeks later, CD19$^+$ splenocytes were harvested from both groups and cultured for 72 hours in the presence or absence of PMA and ionomycin, and then supernatants were collected and IL-10 production was measured by ELISA. Error bars indicate SEM values obtained from mice in each group (n = 3) (*$P < 0.02$ versus PBS). ELISA, enzyme-linked immunosorbent assay.

Phagocytosis of ACs a Prerequisite to Induce Splenic B Cells

We then examined whether ACs interact directly with splenic B cells to induce IL-10 production or indirectly exert their effects after undergoing phagocytosis. For this purpose, we selected MFG-E8 KO mice, which are characterized by impaired uptake of ACs,[23] as the host strain. Syngeneic ACs or the vehicle (PBS) was injected into MFG-E8 KO mice. Three weeks later, CD19$^+$ splenocytes from both groups were cultured in the presence or absence of PMA and ionomycin. Although IL-10 production from B cells were similar in both the AC and PBS groups under the stimulated condition, those from the AC group produced significantly lower levels of IL-10 as compared with B cells from the PBS group under the unstimulated condition (Fig. 4C).

Apoptosis Induced by Reactive Oxygen Species in Circulating Neutrophils During GMA

GMA is used as a therapeutic option for induction therapy for several immune-mediated disorders including IBD, rheumatoid arthritis, and psoriasis.[33–35] Adacolumn is an adsorptive type carrier-based medical device for GMA, and its major components are cellulose acetate beads, which absorb activated granulocytes and monocytes from peripheral blood. The main concept behind the development of the Adacolumn is removal of activated leukocytes for preventing their migration to inflammatory sites. However, the actions of the column are more than just removing leucocytes, as a type of immunomodulation has also been suggested by results of several clinical or basic research studies.[36–38] Reactive oxygen species (ROS) are generated in the Adacolumn by contact between the beads and activated leukocytes, which change the leukocyte cell surface makers to L-selectin^{low}.[26,39] Previous studies have shown that apoptosis develops in leukocytes characterized by those markers.[40] Thus, we speculated that a considerable number of apoptotic leukocytes induced by ROS in the Adacolumn re-enter the body and contribute to the efficacy of GMA.

We used a rabbit immune arthritis model for investigating ROS-induced apoptosis of circulating neutrophils during GMA

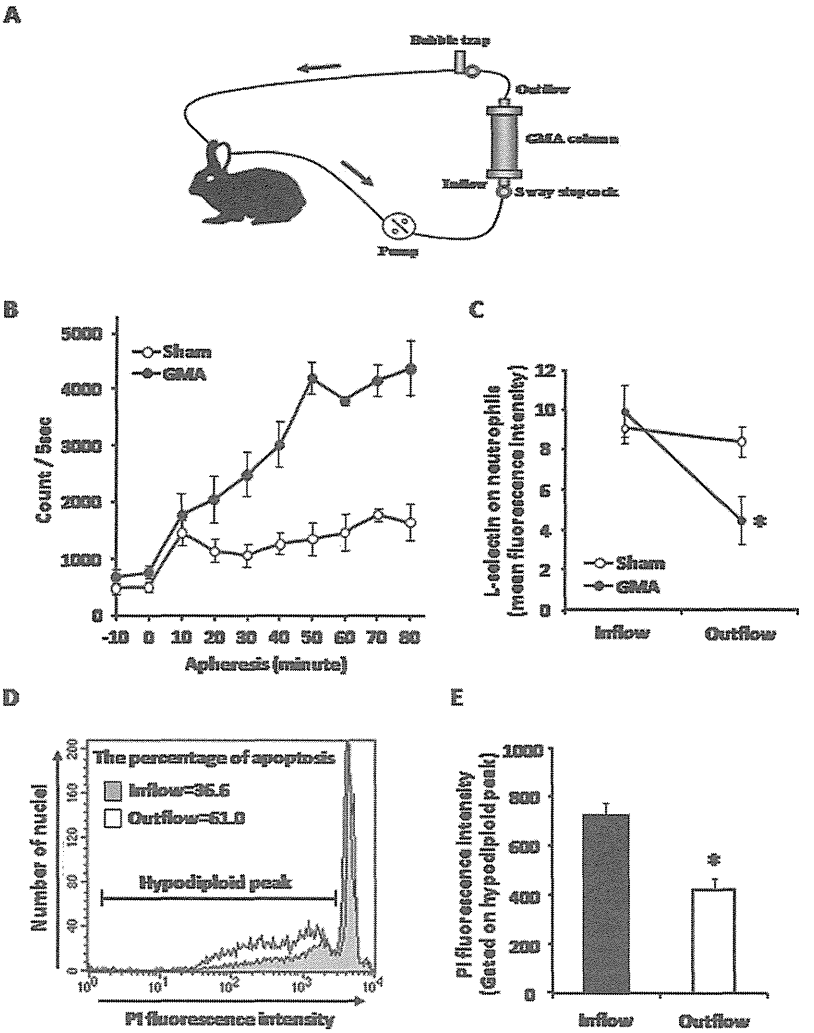

FIGURE 5. Superoxide anion radical produced in the GMA column and shedding of L-selectin and enhancement of apoptosis in neutrophils from GMA column outflow. A, GMA in rabbits with arthritis using a mini GMA column. B, Each rabbit was continuously infused with 185 μM of MCLA at a flow rate of 10 mL/h starting at 10 minutes before initiation of GMA (closed circle, n = 4) or as sham (open circle, n = 4) apheresis. The columns were placed inside the chamber of a photon counting unit shielded from light and apheresis was performed. The amount of the superoxide anion radical O_2^- was measured by directly counting the photons emitted by MCLA on reaction with O_2^-. Error bars indicate SEM values obtained from mice in each group. C, EDTA-blood samples from column inflow and outflow were labeled with an FITC-conjugated anti–L-selectin monoclonal antibody (LAM1-3). Closed circle: GMA (n = 11) (*$P < 0.0001$ versus inflow); open circle: sham (n = 11). Error bars indicate SEM values obtained from mice in each group. Inflow and outflow were compared using a Wilcoxon signed-rank test. D, A rabbit experimental arthritis model received GMA treatment. One hour after initiation of GMA, blood was collected from the GMA column inflow and outflow to isolate neutrophils. Cytometric analyses of PI-stained neutrophil nuclei were conducted after 18 hours of in vitro culture. Each overlay histogram shown is representative of 3 experiments. The proportion of apoptotic neutrophils was analyzed by gating on a broad hypodiploid peak. E, Geometric mean PI fluorescence intensity of the hypodiploid peak from neutrophils in the inflow and outflow from the GMA column were compared using a paired *t* test (n = 3) (*$P < 0.02$ versus inflow). Error bars indicate SEM values obtained from mice in each group. PI, propidium iodide.

(Fig. 5A). Photon counts were gradually increased after initiation of GMA, which was not found in a sham apheresis model (Fig. 5B). Furthermore, generation of O_2^- in the column was confirmed by infusion of superoxide dismutase into the column. Thereafter, photon counts were reduced to the baseline level (data not shown). Also, a significant decrease in L-selectin expression on neutrophils was observed in the GMA outflow (Fig. 5C), whereas hypodiploid apoptotic neutrophils were also significantly increased in the outflow (Fig. 5D, E). These results suggest that apoptosis is induced by ROS in circulating neutrophils during GMA and a considerable number of apoptotic neutrophils re-enter the body.

H_2O_2-induced Apoptotic Neutrophils Ameliorate Mice Colitis

We selected mice colitis model to reveal immunomodulatory effect of apoptotic neutrophils generated during GMA therapy. To mimic apoptotic neutrophils generated during GMA therapy, we isolated PECs, containing 65% to 85% neutrophils,[31] from AKR mice and induced them to undergo apoptosis by exposure to H_2O_2, one kind of ROS. That treatment changed the neutrophil surface marker to L-selectin^{low}, which was similar to the change found in cells after contact with the Adacolumn beads (Fig. 6A). In addition, we confirmed apoptosis induction in those cells by Annexin V staining (Fig. 6B). Next, we replaced the apoptotic thymocytes with APECs and investigated the anti-inflammatory effects of intravenous injection of APECs in the SCID chronic colitis model in the presence of cotransferred CD19$^+$ splenocytes (Fig. 6C). The inflammatory parameters BW loss (Fig. 6D), histological scores for the large intestine (Fig. 6E, F), and expression levels of proinflammatory cytokines in the colitis mice were less severe in the AC group as compared with the PBS group (Fig. 6G).

DISCUSSION

In this study, injection of ACs ameliorated chronic intestinal inflammation in mice only in the presence of cotransferred whole B cells and not in their absence. Furthermore, the ameliorative effect of ACs was lost when whole B cells were replaced by IL-10–producing CD19hiCD1dhi-depleted B cells. In addition, injection of ACs induced IL-10 production in host splenic B cells only in the presence of normal phagocytic function. These novel findings show that ACs have potential to activate the pre-existing Breg population into IL-10 secreting active mode and/or induce differentiation of immature B cells into Bregs. In addition, we showed the possibility that AC-mediated inhibition of colitis may be an anti-inflammatory mechanism of GMA for IBD.

Potent inducers of AC death such as ultraviolet irradiation and x-ray exposure ameliorate inflammatory diseases,[41,42] whereas sepsis-induced apoptosis suppresses delayed-type hypersensitivity in mice.[43] Recently, adoptively transferred ACs were reported to protect mice from autoimmune diseases, including collagen-induced arthritis[11] and experimental autoimmune encephalitis.[44] In addition, transfusion of donor ACs prolonged heart allograft survival in rats[45] and skin allograft survival in a mice model.[46] According to those reports, ACs can exert their protective effect in a variety of immune-mediated disorders regardless of whether apoptosis was induced in vivo or ACs induced with an in vitro method were administered in an adoptive manner. Although the positive impact of ACs has been demonstrated in autoimmune inflammation and allograft survival enhancement, there is no report of the role of ACs in chronic intestinal inflammation.

In this study, we investigated the effects of ACs in an adoptive transfer model of mice colitis and found that their injection had no effects, positive or negative, on the severity of colitis in SCID mice. Previous studies have revealed that most CD4$^+$ T cells isolated from SAMP1 mice are already activated.[47] In addition, Tregs have been reported to be dysfunctional in SMAP1 mice.[48] These findings might explain why ACs failed to reduce colitis severity in the present model.

Our recent findings showed that Bregs expressing IL-10 play an important role in the pathogenesis of ileitis in SAMP1 mice.[49] Furthermore, cotransferred Breg-depleted B cells exacerbated colitis in SCID mice transferred with SAMP1 CD4$^+$ T cells.[22] The role of Bregs has also been shown in several colitis models such as TCR-α–deficient and Gαi2-deficient mice,[50–52] and they are considered to contribute to immune modulation in the intestinal tract. Because SCID mice do not have mature B cells, we speculated that ACs may play an important role to reduce the severity of chronic colitis cofunctioning with Bregs. The present results indicated that colitis activity was significantly lower in mice after cotransfer of whole CD19$^+$ B cells and ACs as compared with that in colitis mice after cotransfer of whole CD19$^+$ B cells and PBS. We recently reported that IL-10–producing Bregs were enriched in a population of CD19hiCD1dhi B cells.[22] To further confirm the role of Bregs in the beneficial effects of ACs, we cotransferred CD19hiCD1dhi-depleted B cells and ACs to colitis mice. Our results indicated that depletion of Bregs canceled out the effect of ACs, suggesting that the anti-inflammatory activities of ACs are dependent on the presence of Bregs.

Several reports have shown that intravenous injection delivers ACs to the spleen,[11,53] whereas it is known that systemic tolerance to ACs is dependent on splenic function.[54] Thus, we focused on the interaction of injected ACs with splenic B cells in vivo. Our results demonstrated an increased frequency of IL-10–producing B cells in AC-injected mice as compared with that of PBS-injected mice in both the presence and absence of stimulation. Furthermore, splenic CD19$^+$ B cells from the AC group produced significantly higher levels of IL-10 as compared with those from the PBS group under basal and activated conditions. The present finding that AC-induced IL-10 production in splenic B cells in vivo is consistent with other recent findings.[11,44] Gray et al[11] reported that inhibition of IL-10 in vivo reversed the beneficial effect of ACs in collagen-induced arthritis, whereas collagen-induced arthritis was reported to exacerbate in IL-10–deficient mice.[55,56] IL-10 is a multifunctional cytokine with an ability to inhibit activation and effector functions of various immune cells.[57] However, it remains unknown whether the anti-inflammatory effects of ACs are simply dependent on IL-10 production by Bregs. The mechanisms by which regulatory function can be imparted to B cells by interaction with ACs require further investigation.

We also investigated whether injected ACs interacted directly or indirectly with splenic B cells after engulfment by splenic phagocytes to induce IL-10 production. As the host strain, we used MFG-E8 KO mice, which are characterized by impaired uptake of ACs.[23] Our results indicated that splenic CD19$^+$ B cells

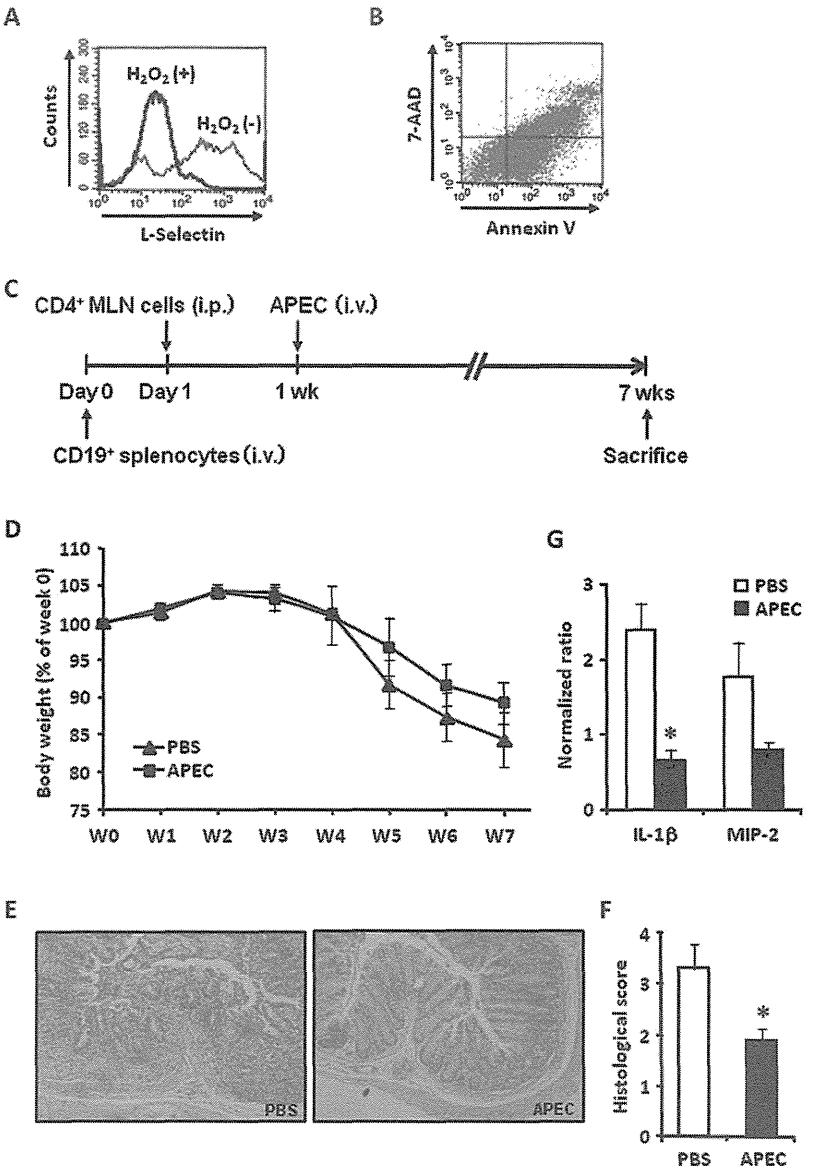

FIGURE 6. APECs ameliorated intestinal inflammation in SAMP1 $CD4^+$ MLN T-cell–induced chronic colitic mice when cotransferred with $CD19^+$ splenocytes. A, Flow cytometric analysis of L-selectin expression on H_2O_2-treated or untreated PECs from AKR mice. PEC suspensions were treated with lysing solution to remove red blood cells. PECs (2×10^6 cells per milliliter) were treated with 500 μM H_2O_2 for 1 hour at 37°C, and then stained with anti-CD62L MoAb for flow cytometric analysis. B, H_2O_2-treated PECs were subjected to flow cytometry after staining with annexin V and 7-AAD. C, Protocol for cotransfer of $CD19^+$ splenocytes and APECs in SAMP1 $CD4^+$ MLN T-cell–induced chronic colitic SCID mice. Purified whole $CD19^+$ splenocytes (2×10^6 cells per mouse) derived from AKR mice and SAMP1 $CD4^+$ MLN T cells (5×10^5 cells per mouse) were injected intravenously on day 0 and intraperitoneally on day 1, respectively, into 8- to 10-week-old SCID mice. D, Effects of APECs on BW changes after injection of $CD19^+$ splenocytes into SAMP1 $CD4^+$ MLN T-cell–induced chronic colitic mice. The APEC group (squares) was given an intravenous injection of APECs (1×10^7 cells per mouse) on week 1, whereas the control group received the vehicle alone (triangle). Data are expressed as serial changes in percentage of weight change over a 7-week period. Error bars indicate SEM values obtained from mice in each group (n = 5). E, Representative images of histological changes in large intestines at 7 weeks after injection of $CD19^+$ splenocytes and SAMP1 $CD4^+$ MLN T cells with or without APECs. F, Mean values of intestinal histological scores in each experimental group. Error bars indicate SEM values obtained from mice in each group (n = 5) (*$P < 0.04$ versus PBS). G, Gene expressions of IL-1β and MIP-2 in large intestines in each experimental group. Error bars indicate SEM values obtained from mice in each group (n = 5) (*$P < 0.03$ versus PBS).

from both the AC and PBS groups produced similar levels of IL-10 in both the presence and absence of stimulation. This novel finding demonstrated that phagocytosis of ACs is a prerequisite for induction of IL-10–producing B cells. Ravishankar et al[46] reported that AC-mediated allograft tolerance requires $CD169^+$ macrophages located in the splenic marginal zone. Deficiency in removal of ACs can lead to autoimmune disorders such as systemic lupus erythematosus.[8,58] AC-induced tolerance in allogeneic heart transplants was reported to be prevented by administrations of gadolinium chloride, which disrupts phagocyte function, and annexin V, which blocks the binding of exposed phosphatidylserine to its receptor on phagocytes.[45] Thus, without being phagocytosed, ACs are unable to induce immune tolerance. We speculated that phagocytosis of injected ACs plays a decisive role in influencing generation of IL-10–producing Bregs, which in turn determines the outcome of adoptively transferred colitis. Recent studies have revealed that IL-10 production by B cells in vitro requires direct contact with ACs.[11,44] Additional studies of the direct interactions between ACs and B cells in vivo are necessary to clarify this point.

GMA, a type of cytapheresis, is used as induction therapy for IBD in Japan and European countries.[59–61] Its efficacy is dependent on removing circulating activated leukocytes with an Adacolumn device, which prevents their migration to inflammatory sites in the intestine. Postmarketing surveillance in Japan of 697 patients with ulcerative colitis treated at 53 medical institutions over 7 years from 1999 to 2006 was undertaken by the manufacturer, which showed satisfactory clinical efficacy and safety.[59] Although the efficacy of GMA is similar to that of other leukocytapheresis methods, and the average adsorption rate of leukocytes to an Adacolumn is relatively low (30%–40%) as compared with other methods. Thus, we considered that a considerable number of leukocytes re-enter the body after contact with the Adacolumn beads, which may be related to the anti-inflammatory effects of GMA. Experimental results have also revealed that ROS generated in the Adacolumn change the leukocyte cell surface markers to L-$selectin^{low}$ and induce those cells to undergo apoptosis. Inbred strains of mice including AKR are deficient in components of complement,[62] whereas deposition of complement fragments, such as C3bi, as ligand for CR3 onto Adacolumn beads is one of the requirements for effective removal of activated leukocytes.[27] Thus, we could not use mice apoptotic leukocytes induced by the Adacolumn beads. In this study, we examined the effects of injected H_2O_2-induced apoptotic leukocytes in an SCID colitis model cotransferred with whole B cells and found that injection of APECs reduced colitis severity, suggesting that apoptotic leukocytes induced by ROS generated in the Adacolumn may contribute to the efficacy of GMA. To confirm the anti-inflammatory mechanisms of GMA associated with induction and efficacy of ACs, additional experiments are required.

In this study, we demonstrated that injection of ACs reduced the severity of mice colitis in the presence of IL-10–producing CD19hiCD1dhi B cells. We also speculate that this ameliorative effect of ACs might be one of the anti-inflammatory mechanisms of GMA for IBD. However, it remains unknown whether ACs activate pre-existing Bregs or cause immature B cells to differentiate into Bregs. Elucidation of the detailed mechanisms of AC-mediated anti-inflammatory effects may lead to a novel therapeutic strategy for IBD.

REFERENCES

1. Vaux DL. Toward an understanding of the molecular mechanisms of physiological cell death. *Proc Natl Acad Sci U S A.* 1993;90:786–789.
2. Savill J, Fadok V, Henson P, et al. Phagocyte recognition of cells undergoing apoptosis. *Immunol Today.* 1993;14:131–136.
3. Ferguson TA, Stuart PM, Herndon JM, et al. Apoptosis, tolerance, and regulatory T cells—old wine, new wineskins. *Immunol Rev.* 2003;193:111–123.
4. Green DR, Ferguson T, Zitvogel L, et al. Immunogenic and tolerogenic cell death. *Nat Rev Immunol.* 2009;9:353–363.
5. Griffith TS, Kazama H, VanOosten RL, et al. Apoptotic cells induce tolerance by generating helpless $CD8^+$T cells that produce TRAIL. *J Immunol.* 2007;178:2679–2687.
6. Ferguson TA, Herndon J, Elzey B, et al. Uptake of apoptotic antigen-coupled cells by lymphoid dendritic cells and cross-priming of CD8(+) T cells produce active immune unresponsiveness. *J Immunol.* 2002;168:5589–5595.
7. Steinman RM, Turley S, Mellman I, et al. The induction of tolerance by dendritic cells that have captured apoptotic cells. *J Exp Med.* 2000;191:411–416.
8. Bijl M, Reefman E, Horst G, et al. Reduced uptake of apoptotic cells by macrophages in systemic lupus erythematosus: correlates with decreased serum levels of complement. *Ann Rheum Dis.* 2006;65:57–63.
9. Fadok VA, Bratton DL, Konowal A, et al. Macrophages that have ingested apoptotic cells in vitro inhibit proinflammatory cytokine production through autocrine/paracrine mechanisms involving TGF-beta, PGE2, and PAF. *J Clin Invest.* 1998;101:890–898.
10. Liu K, Iyoda T, Saternus M, et al. Immune tolerance after delivery of dying cells to dendritic cells in situ. *J Exp Med.* 2002;196:1091–1097.
11. Gray M, Miles K, Salter D, et al. Apoptotic cells protect mice from autoimmune inflammation by the induction of regulatory B cells. *Proc Natl Acad Sci U S A.*2007;104:14080–14085.
12. Notley CA, Brown MA, Wright GP, et al. Natural IgM is required for suppression of inflammatory arthritis by apoptotic cells. *J Immunol.* 2011;186:4967–4972.
13. Chen Y, Khanna S, Goodyear CS, et al. Regulation of dendritic cells and macrophages by an anti-apoptotic cell natural antibody that suppresses TLR responses and inhibits inflammatory arthritis. *J Immunol.* 2009;183:1346–1359.
14. Voll RE, Herrmann M, Roth EA, et al. Immunosuppressive effects of apoptotic cells. *Nature.* 1997;390:350–351.
15. Marteau P. Inflammatory bowel disease. *Endoscopy.* 2000;32:131–137.
16. Podolsky DK. Inflammatory bowel disease. *N Engl J Med.* 1991;325:928–937.
17. Satsangi J, Jewell D, Parkes M, et al. Genetics of inflammatory bowel disease. A personal view on progress and prospects. *Dig Dis.* 1998;16:370–374.
18. Satsangi J, Welsh KI, Bunce M, et al. Contribution of genes of the major histocompatibility complex to susceptibility and disease phenotype in inflammatory bowel disease. *Lancet.* 1996;347:1212–1217.
19. Duerr RH. Genetics of inflammatory bowel disease. *Inflamm Bowel Dis.* 1996;2:48–60.
20. Papadakis KA, Targan SR. Current theories on the causes of inflammatory bowel disease. *Gastroenterol Clin North Am.* 1999;28:283–296.
21. Noguchi M, Hiwatashi N, Liu Z, et al. Secretion imbalance between tumour necrosis factor and its inhibitor in inflammatory bowel disease. *Gut.* 1998;43:203–209.
22. Oka A, Ishihara S, Mishima Y, et al. Role of regulatory B cells in chronic intestinal inflammation: association with pathogenesis of Crohn's disease. *Inflamm Bowel Dis.* 2014;20:315–328.

23. Hanayama R, Tanaka M, Miyasaka K, et al. Autoimmune disease and impaired uptake of apoptotic cells in MFG-E8-deficient mice. *Science.* 2004;304:1147–1150.
24. Burns RC, Rivera-Nieves J, Moskaluk CA, et al. Antibody blockade of ICAM-1 and VCAM-1 ameliorates inflammation in the SAMP-1/Yit adoptive transfer model of Crohn's disease in mice. *Gastroenterology.* 2001;121:1428–1436.
25. Pettipher EA, Henderson B, Moncada S, et al. Leucocyte infiltration and cartilage proteoglycan loss in immune arthritis in the rabbit. *Br J Pharmacol.* 1988;98:176–196.
26. Kashiwagi N, Nakano M, Saniabadi AR, et al. Anti-inflammatory effect of granulocyte and monocyte adsorption apheresis in a rabbit model of immune arthritis. *Inflammation.* 2002;26:199–205.
27. Takeda Y, Shiobara N, Saniabadi AR, et al. Adhesion dependent release of hepatocyte growth factor and interleukin-1 receptor antagonist from human granulocytes and monocytes: evidence for the involvement of plasma IgG, complement C3 and b2 integrin. *Inflamm Res.* 2004;53: 277–283.
28. Uehara K, Maruyama N, Huang C, et al. The first application of a chemiluminescence probe for detecting O_2-production in vitro from Kupffer cells stimulated by phorbol myristate acetate. *FEBS Lett.* 1993;335:167–170.
29. Roberts RL, Gallin JI. Rapid method for isolation of normal human peripheral blood eosinophils on discontinuous Percoll gradients and comparison with neutrophils. *Blood.* 1985;65:433–440.
30. Dransfield I, Buckle AM, Savill JS, et al. Neutrophil apoptosis is associated with a reduction in CD16 (FcγRIII) expression. *J Immunol.* 1994; 153:1254–1263.
31. Kannan Y, Ushio H, Koyama H, et al. 2.5S nerve growth factor enhances survival, phagocytosis, and superoxide production of murine neutrophils. *Blood.* 1991;77:1320–1325.
32. Kannan Y, Usami K, Okada M, et al. Nerve growth factor suppresses apoptosis of murine neutrophils. *Biochem Biophys Res Commun.* 1992; 186:1050–1056.
33. Sacco R, Romano A, Mazzoni A, et al. Granulocytapheresis in steroid-dependent and steroid-resistant patients with inflammatory bowel disease: a prospective observational study. *J Crohns Colitis.* 2013;7:e692–e697.
34. Fukuchi T, Nakase H, Matsuura M, et al. Effect of intensive granulocyte and monocyte adsorptive apheresis in patients with ulcerative colitis positive for cytomegalovirus. *J Crohns Colitis.* 2013;7:803–811.
35. Ikeda S, Takahashi H, Suga Y, et al. Therapeutic depletion of myeloid lineage leukocytes in patients with generalized pustular psoriasis indicates a major role for neutrophils in the immunopathogenesis of psoriasis. *J Am Acad Dermatol.* 2013;68:609–617.
36. Diepolder HM, Kashiwagi N, Teuber G, et al. Leucocytapheresis with Adacolumn enhances HCV-specific proliferative responses in patients infected with hepatitis C virus genotype 1. *J Med Virol.* 2005;77:209–215.
37. Noguchi A, Watanabe K, Narumi S, et al. The production of interferon-gamma-inducible protein 10 by granulocytes and monocytes is associated with ulcerative colitis disease activity. *J Gastroenterol.* 2007;42:947–956.
38. Kashiwagi N, Hirata I, Kasukawa R. A role for granulocyte and monocyte apheresis in the treatment of rheumatoid arthritis. *Ther Apher.* 1998;2: 134–141.
39. Ramlow W, Emmrich J, Ahrenholz P, et al. In vitro and in vivo evaluation of Adacolumn cytapheresis in healthy subjects. *J Clin Apher.* 2005;20:72–80.
40. Dransfield I, Stocks SC, Haslett C. Regulation of cell adhesion molecule expression and function associated with neutrophil apoptosis. *Blood.* 1995;85:3264–3273.
41. Abel EA. Phototherapy. *Dermatol Clin.* 1995;13:841–849.
42. Trott KR. Therapeutic effects of low radiation doses. *Strahlenther Onkol.* 1994;170:1–12.
43. Unsinger J, Kazama H, McDonough JS, et al. Sepsis-induced apoptosis leads to active suppression of delayed-type hypersensitivity by $CD8^+$ regulatory T cells through a TRAIL-dependent mechanism. *J Immunol.* 2010;184:6766–6772.
44. Miles K, Heaney J, Sibinska Z, et al. A tolerogenic role for Toll-like receptor 9 is revealed by B-cell interaction with DNA complexes expressed on apoptotic cells. *Proc Natl Acad Sci U S A.* 2012;109:887–892.
45. Sun E, Gao Y, Chen J, et al. Allograft tolerance induced by donor apoptotic lymphocytes requires phagocytosis in the recipient. *Cell Death Differ.* 2004;11:1258–1264.
46. Ravishankar B, Shinde R, Liu H, et al. Marginal zone $CD169^+$ macrophages coordinate apoptotic cell-driven cellular recruitment and tolerance. *Proc Natl Acad Sci U S A.* 2014;111:4215–4220.
47. Kosiewicz MM, Nast CC, Krishnan A, et al. Th1-type responses mediate spontaneous ileitis in a novel murine model of Crohn's disease. *J Clin Invest.* 2001;107:695–702.
48. Ishikawa D, Okazawa A, Corridoni D, et al. Tregs are dysfunctional in vivo in a spontaneous murine model of Crohn's disease. *Mucosal Immunol.* 2013;6:267–275.
49. Mishima Y, Ishihara S, Aziz MM, et al. Decreased production of interleukin-10 and transforming growth factor-β in Toll-like receptor-activated intestinal B cells in SAMP1/Yit mice. *Immunology.* 2010;131:473–487.
50. Mizoguchi A, Mizoguchi E, Smith RN, et al. Suppressive role of B cells in chronic colitis of T cell receptor alpha mutant mice. *J Exp Med.* 1997; 186:1749–1756.
51. Wei B, Velazquez P, Turovskaya O, et al. Mesenteric B cells centrally inhibit $CD4^+$ T cell colitis through interaction with regulatory T cell subsets. *Proc Natl Acad Sci U S A.* 2005;102:2010–2015.
52. Brummel R, Lenert P. Activation of marginal zone B cells from lupus mice with type A(D) CpG-oligodeoxynucleotides. *J Immunol.* 2005;174: 2429–2434.
53. Morelli AE, Larregina AT, Shufesky WJ, et al. Internalization of circulating apoptotic cells by splenic marginal zone dendritic cells: dependence on complement receptors and effect on cytokine production. *Blood.* 2003; 101:611–620.
54. Streilein JW, Niederkorn JY. Induction of anterior chamber-associated immune deviation requires an intact, functional spleen. *J Exp Med.* 1981;153:1058–1067.
55. Finnegan A, Kaplan CD, Cao Y, et al. Collagen-induced arthritis is exacerbated in IL-10-deficient mice. *Arthritis Res Ther.* 2003;5:R18–R24.
56. Johansson AC, Hansson AS, Nandakumar KS, et al. IL-10-deficient B10. Q mice develop more severe collagen-induced arthritis, but are protected from arthritis induced with anti-type II collagen antibodies. *J Immunol.* 2001;167:3505–3512.
57. Moore KW, de Waal Malefyt R, Coffman RL, et al. Interleukin-10 and the interleukin-10 receptor. *Annu Rev Immunol.* 2001;19:683–765.
58. Ginaldi L, Martinis MD, D'Ostilio A, et al. Cell proliferation and apoptosis in the immune system in the elderly. *Immunol Res.* 2000;21:31–38.
59. Hibi T, Sameshima Y, Sekiguchi Y, et al. Treating ulcerative colitis by Adacolumn therapeutic leucocytapheresis: clinical efficacy and safety based on surveillance of 656 patients in 53 centres in Japan. *Dig Liver Dis.* 2009;41:570–577.
60. Vecchi M, Vernia P, Riegler G, et al. Therapeutic landscape for ulcerative colitis: where is the Adacolumn® system and where should it be? *Clin Exp Gastroenterol.* 2013;6:1–7.
61. Linton L, Karlsson M, Grundström J, et al. HLA-DR(hi) and CCR9 define a pro-inflammatory monocyte subset in IBD. *Clin Transl Gastroenterol.* 2012;3:e29.
62. Wetsel RA, Fleischer DT, Haviland DL. Deficiency of the murine fifth complement component (C5). *J Biol Chem.* 1990;265:2435–2440.

INTERNAL MEDICINE

□ ORIGINAL ARTICLE □

Relationship between Esophageal Cardiac Glands and Gastroesophageal Reflux Disease

Kozue Hanada[1], Kyoichi Adachi[1], Tomoko Mishiro[1], Shino Tanaka[1], Yoshiko Takahashi[1], Kazuaki Yoshikawa[1] and Yoshikazu Kinoshita[2]

Abstract

Objective The role of esophageal cardiac glands has not been fully determined. This study was performed to clarify the protective role of esophageal cardiac glands against the development of gastroesophageal reflux disease (GERD).

Methods The subjects included 2,656 Japanese individuals who visited our institution for a detailed medical checkup. GERD symptoms were assessed using the Japanese version of the Carlsson-Dent self-administered questionnaire (QUEST) and an upper gastrointestinal endoscopy examination in each subject. The presence of reflux esophagitis, size of diaphragmatic hiatus, degree of gastric mucosal atrophy and existence of visible esophageal cardiac glands in the distal esophagus, based on the detection of yellowish elevated areas, were determined using endoscopy.

Results Esophageal cardiac glands were observed in 355 cases (13.4%). Reflux esophagitis was significantly less frequent in the cases with esophageal cardiac glands than in those without. The esophageal cardiac glands were mainly located on the left-posterior side of the esophageal wall of the distal esophagus. A multiple regression analysis showed that the presence of esophageal cardiac glands was an independent factor for preventing reflux esophagitis. On the other hand, the existence of these glands did not correlate with the presence of GERD symptoms (QUEST score of 6 or more).

Conclusion The presence of visible esophageal cardiac glands may have a protective role against the development of reflux esophagitis.

Key words: esophageal cardiac gland, reflux esophagitis, GERD, QUEST, endoscopy

(Intern Med 54: 91-96, 2015)
(DOI: 10.2169/internalmedicine.54.3179)

Introduction

Gastroesophageal reflux disease (GERD) is characterized by the presence of esophageal mucosal injury or reflux symptoms caused by abnormal reflux of acidic gastric contents into the esophagus (1). The esophageal mucosa is protected from injury from acid reflux by several mechanisms, including salivary secretion, esophageal peristalsis and components of the esophageal mucosal protection system, such as the mucous layer on the surface (2-7). The secretion of mucous from esophageal glands is important for protecting the mucosal surface from the pepsin and protease contained in gastric juices. There are two types of secretory glands in the esophagus: superficial glands located in the proper mucosal layer and deep mucous glands located in the submucosa (8). Superficial mucosal glands are found in limited numbers in the upper esophagus and near the junction with the stomach. Those located in the distal esophagus are tortuous and tubular, lined with cuboidal or columnar epithelial cells, and resemble the cardiac glands of the cardia. Based on this resemblance, superficial mucosal glands in the distal esophagus are called esophageal cardiac glands. These glands are considered to play a protective role against mucosal injury in the lower esophagus caused by reflux of acidic gastric contents.

[1]Health Center, Shimane Environment and Health Public Corporation, Japan and [2]The Second Department of Internal Medicine, Shimane University Faculty of Medicine, Japan
Received for publication April 27, 2014; Accepted for publication June 3, 2014
Correspondence to Dr. Kyoichi Adachi, adachi@kanhokou.or.jp

Esophageal cardiac glands are visualized as yellow elevated areas in the distal esophagus on endoscopy (9, 10). However, the relationship between these glands and GERD has not been fully determined. We conducted this relatively large-scale study in order to clarify the protective role of esophageal cardiac glands against the development of GERD in Japanese subjects.

Materials and Methods

This study was approved by the ethics committee of Shimane University Faculty of Medicine. Written informed consent was obtained from all enrolled subjects, and the study was performed according to the World Medical Association Declaration of Helsinki.

The subjects included individuals who visited the Health Center of Shimane Environment and Health Public Corporation for a detailed medical checkup between April 2011 and March 2012. A majority of the subjects were socially active, productive and socioeconomically middle class individuals. After obtaining written informed consent for enrollment into the study, a precise medical history was taken. Individuals with a history of gastric surgery were not included in this study. Patients who had taken medications such as proton pump inhibitors, H2 receptor antagonists or prokinetic drugs within the preceding three months were excluded. In addition, those who had received eradication therapy for *Helicobacter pylori* (*H. pylori*) infection were excluded, as a relationship between *H. pylori* infection and the presence of esophageal cardiac glands has been suggested (9). The body mass index (BMI) and current smoking and drinking (equivalent to over 50 mL of alcohol per day) habits were also noted.

All subjects underwent an upper gastrointestinal endoscopy examination. Prior to the examination, the presence or absence of reflux symptoms was assessed using the Japanese version of the Carlsson-Dent self-administered questionnaire (QUEST) (11). We defined subjects with a QUEST score of 6 or more as being positive for reflux symptoms, since a cut-off score of 6 has been demonstrated to have higher specificity for the diagnosis of GERD than a score of 4. The endoscopic findings of reflux esophagitis were evaluated using the Los Angeles (LA) classification (12), and individuals with a grade of A, B, C or D were diagnosed as being positive for reflux esophagitis. The size of the diaphragmatic hiatus was also assessed during endoscopic observation of the stomach and categorized into three groups (<1.0, 1.0-2.0, >2 cm). The degree of gastric mucosal atrophy was evaluated endoscopically using the classification of Kimura and Takemoto, according to which gastric mucosal atrophy was classified into six groups (C1, C2, C3, O1, O2, O3) (13). It has been shown that gastric mucosal atrophy progresses from stage C1 to O3 in a successive manner, and this classification has been proven to correlate well with histological features (13). In addition, gastric acid secretion in patients with gastric mucosal atrophy has been demonstrated to decrease successively from stage C1 to O3 (14). In this study, we defined C1-C2 as mild, C3-O1 as moderate and O2-O3 as severe gastric mucosal atrophy.

The presence of esophageal cardiac glands was determined based on the detection of a visible yellowish elevated area on the proximal side of the gastroesophageal junction (9, 10), and the distribution of these lesions was assessed by dividing the findings into four grades (grade 0: absence of esophageal cardiac glands, grade 1: 1-5 spots indicating esophageal cardiac glands, grade 2: continuous transversely extending esophageal cardiac glands involving less than 50% of the esophageal circumference, grade 3: continuous transversely extending esophageal cardiac glands involving at least 50% of the esophageal circumference) (Fig. 1). None of the present subjects had more than five spots indicating esophageal cardiac glands separately existing in the distal esophagus, while those with continuously transversely extending glands (grade 2 and 3) occasionally had a few unconnected esophageal cardiac glands. Esophageal cardiac glands are considered to extend from grade 0 to 3 in a successive manner. The circumferential localization of the esophageal cardiac glands was also investigated. If multiple esophageal cardiac glands were present, their circumferential positions were recorded. In cases involving transversely extending glands, those extending in all directions were counted. In this study, all upper endoscopic examinations were performed by experienced endoscopists (K.H, S.T and K.Y.), and the endoscopic photographs were reviewed by two endoscopists (K.H and K.A.) to determine the existence and location of the esophageal cardiac glands.

The statistical analyses were performed using the chi-squared, Kruskal-Wallis and Mann-Whitney U tests. A multiple logistic regression analysis was conducted to calculate the odds ratios. All calculations were carried out using the Stat View 5.0 software program (Abacus Concepts, Berkeley, USA) for Macintosh, and differences of $p<0.05$ were considered to be statistically significant.

Results

We prospectively enrolled 2,656 subjects (mean age: 51.8±9.2 years, men: 1,835) in this study, and esophageal cardiac glands were endoscopically observed in 355 cases (13.4%). The number of patients with grade 1, 2, and 3 lesions was 258 (9.7%), 47 (1.8%) and 50 (1.9%), respectively. There were no significant differences in regard to age between the grades. Esophageal cardiac glands were more frequently observed in women (17.1% vs. 11.7%). Reflux esophagitis was significantly less frequent in the cases with esophageal cardiac glands than in those without, and no cases of grade 2 or 3 esophageal cardiac glands involved reflux esophagitis. The grade of reflux esophagitis did not differ between the cases with and without esophageal cardiac glands, whereas GERD symptoms showed a tendency to be less frequent in the subjects with esophageal cardiac glands. In addition, the rate of GERD symptoms tended to be lower

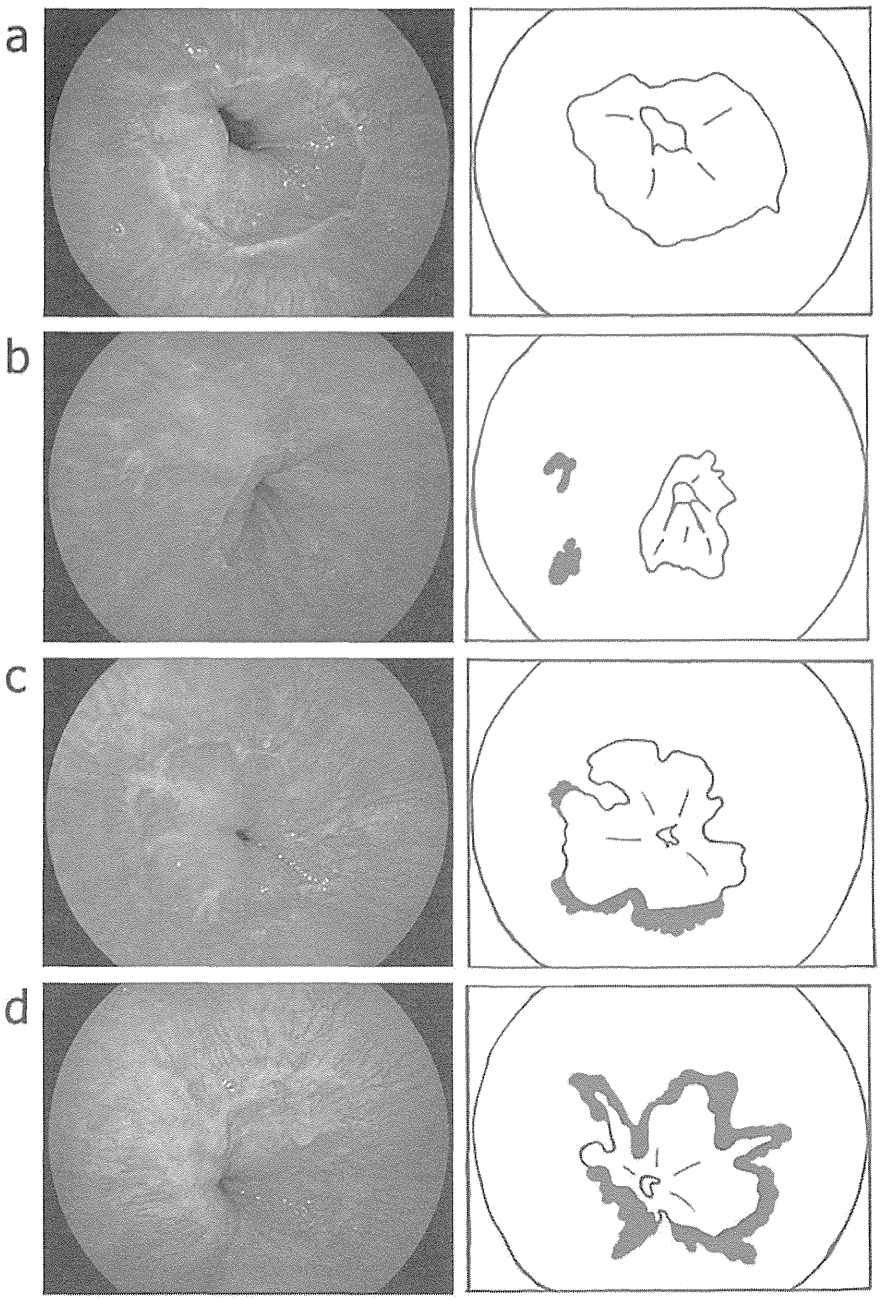

Figure 1. Endoscopic findings and schematic figures of esophageal cardiac glands at the distal end of the esophagus (a: grade 0, b: grade 1, c: grade 2, d: grade 3). The red spots and areas of schema indicate esophageal cardiac glands.

among the reflux esophagitis patients with esophageal cardiac glands than among those without. Furthermore, the degree of gastric mucosal atrophy was significantly increased in the cases with esophageal cardiac glands (Table 1).

The multiple regression analysis was performed by including several factors known to affect the prevalence of reflux esophagitis and GERD symptoms (15-17). A male gender, high BMI, large diaphragmatic hiatus and smoking were shown to be significant risk factors for the presence of reflux esophagitis, while the presence of esophageal cardiac glands and gastric mucosal atrophy were found to be independent factors related to its prevention (Table 2). The multiple regression analysis also showed that a high BMI, severe gastric mucosal atrophy, large diaphragmatic hiatus and smoking were significantly correlated with the occurrence of GERD symptoms. The odds ratio for the presence of esophageal cardiac glands in relation to the development of GERD symptoms was 0.909, which was not statistically significant (Table 3).

We also investigated the circumferential localization of the esophageal cardiac glands in the 355 cases and found that the lesions were mainly located on the left-posterior side of the esophageal wall of the distal esophagus (Fig. 2).

not be explained by the present results. However, the role of esophageal cardiac glands, particularly with regard to the occurrence of GERD, has yet to be determined.

In this study, we investigated the relationship between the presence of endoscopically determined esophageal cardiac glands and the incidence of GERD. Our results demonstrated that these lesions play a protective role against esophageal mucosal injury in the distal esophagus. However, they do not inhibit the development of GERD symptoms. Previously, Yagi and co-workers investigated the prevalence of esophageal cardiac glands in patients with erosive esophagitis and nonerosive reflux disease (NERD) (10) and found that the prevalence of esophageal cardiac glands in patients with NERD is significantly higher than that observed in patients with erosive esophagitis. According to the findings of that and the present study, we conclude that esophageal cardiac glands have a protective effect against injury to the squamous epithelium in the distal esophagus caused by the reflux of acidic gastric contents. On the other hand, GERD symptoms were found to occur irrespective of the presence or absence of these lesions in the current study. Esophageal mucosal injury caused by acidic gastric reflux primarily occurs at the distal end of the esophagus. Esophageal cardiac glands also exist in the distal esophagus, and agents secreted from these glands may provide protection against esophageal mucosal injury. However, acidic reflux contents may stimulate the portion of the esophageal mucosa not covered with mucous secreted from esophageal cardiac glands, thus inducing reflux symptoms. In addition, the acid-neutralizing function of esophageal cardiac glands may not be strong enough to prevent the occurrence of GERD symptoms. Furthermore, several other mechanisms may also influence the development of GERD symptoms, as such symptoms have also been reported to be caused by non-acidic and gas reflux, duodenal juice reflux, esophageal hypersensitivity to acid, esophageal wall distension, esophageal motility abnormalities, sustained esophageal contractions, psychological conditions and others (18-24).

An interesting observation in this study is that the esophageal cardiac glands were found to be primarily located on the left-posterior side of the esophageal wall, which is opposite the main site of mucosal injury in patients with LA-classification A and B grade reflux esophagitis (25, 26). The circumferential localization of mucosal injury in cases of A and B grade reflux esophagitis was shown to largely fit the direction of prolonged acid exposure in a study that used a recently developed 8-channel device with radially arrayed pH sensors (27). Therefore, the direction of esophageal mucosal injury in patients with reflux esophagitis is influenced by the presence of esophageal cardiac glands, which may have an acid-neutralizing function. A future study utilizing circumferential esophageal pH monitoring testing is needed to clarify the acid-neutralizing function of esophageal cardiac glands.

There are several limitations associated with our study. For example, we used endoscopy only to determine the presence of esophageal cardiac glands. Previously, Yagi and coworkers demonstrated that esophageal cardiac glands were histologically observed in the biopsy specimens of 30 of 38 patients with yellowish elevated areas on the most distal squamous epithelium (9). Although the presence of yellowish elevated areas in the distal esophagus is considered to indicate the existence of esophageal cardiac glands, invisible esophageal cardiac glands may also be present at the distal end of the esophagus, where they may play a protective role against esophageal mucosal injury. On the other hand, some yellowish elevated areas may not be esophageal cardiac glands. Therefore, detailed histological studies of surgically resected esophageal specimens, including comparisons with preoperative endoscopic findings, are required to clarify whether invisible esophageal cardiac glands exist. In addition, we did not investigate the incidence of *H. pylori* infection in this study. *H. pylori* infection has repeatedly been demonstrated to cause gastric mucosal atrophy and have a preventive effect against the development of reflux esophagitis (28-32). Therefore, there is a possibility that both hypertrophic changes in esophageal cardiac glands and reductions in reflux esophagitis are induced by *H. pylori* infection. A long-term endoscopy study is thus needed to clarify the conditions under which visible esophageal cardiac glands are formed and develop and to examine the relationship between the expansion of these lesions and the ability to cure esophageal mucosal injury at the distal end of the esophagus.

In conclusion, our findings demonstrate that esophageal cardiac glands may have a protective role against esophageal mucosal injury caused by acidic gastric contents.

The authors state that they have no Conflict of Interest (COI).

References

1. Vakil N, van Zanten SV, Kahrilas P, Dent J, Jones R. The Montreal definition and classification of gastroesophageal reflux disease global evidence-based consensus. Am J Gastroenterology **101**: 1900-1920, 2006.
2. Dodds WJ, Hogan WJ, Helm JF, Dent J. Pathogenesis of reflux esophagitis. Gastroenterology **81**: 376-394, 1981.
3. Korsten MA, Rosman AS, Fishbein S, Shlein RD, Goldberg HE, Biener A. Chronic xerostomia increases esophageal acid exposure and is associated with esophageal injury. Am J Med **90**: 701-706, 1991.
4. Sonnenberg A, Steinkamp U, Weise A, et al. Salivary secretion in reflux esophagitis. Gastroenterology **83**: 889-895, 1982.
5. Kahrilas PJ, Dodds WJ, Hogan WJ, Kern M, Arndorfer RC, Reece A. Esophageal peristaltic dysfunction in peptic esophagitis. Gastroenterology **91**: 897-904, 1986.
6. Kahrilas PJ, Dodds WJ, Hogan WJ. Effect of peristaltic dysfunction on esophageal volume clearance. Gastroenterology **94**: 73-80, 1988.
7. Orlando RC. Review article: oesophageal mucosal resistance. Aliment Pharmacol Ther **12**: 191-197, 1998.
8. Fawcett DW. Esophageal glands. In: Bloom & Fawcett Textbook of Histology. Chapman & Hall, New York/London, 1998: 597.
9. Yagi K, Aruga Y, Nakamura A, Sekine A. An endoscopic and

Table 1. Characteristics of Study Subjects

	Esophageal cardiac glands				p value
	Grade 0	Grade 1	Grade 2	Grade 3	
Number of cases	2301	258	47	50	
Age (mean ± SD)	51.7±9.3	52.0±9.3	53.0±9.4	53.4±7.9	0.519
Male/female	1620/681	152/106	31/16	32/18	0.002
Reflux esophagitis (+)	263 (11.4)	9 (3.5)	0 (0)	0 (0)	<0.001
LA grade-A/B/C	139/80/4	4/5/0			0.467
GERD symptoms (+)	787 (34.2)	81 (31.4)	14 (29.8)	12 (24.0)	0.348
in cases with RE	137 (52.1)	2 (22.2)			0.078
Gastric mucosal atrophy					<0.001
mild	1620 (70.4)	144 (55.8)	8 (17.0)	6 (12.0)	
moderate	548 (23.8)	79 (30.6)	20 (42.6)	21 (42.0)	
severe	133 (5.8)	35 (13.6)	19 (40.4)	23 (46.0)	

Values in parentheses show percentage of cases in each group.
Extension of esophageal cardiac glands was assessed by dividing into 4 grades (grade 0: absence of esophageal cardiac gland, grade 1: 1-5 spots of esophageal cardiac glands, grade 2: continuous transverse extent of esophageal cardiac glands but which involves less than 50% of esophageal circumference, grade 3: continuous transverse extent of esophageal cardiac glands but which involves at least 50% of esophageal circumference).
Reflux esophagitis (RE) (+): grade A-D in Los Angeles (LA) classification.
GERD symptoms (+): QUEST score ≥6.
Gastric mucosal atrophy was evaluated using the classification of Kimura and Takemoto (C1-C2: mild, C3-O1: moderate, O2-O3: severe gastric mucosal atrophy).
p value indicates the difference between the groups.

Table 2. Multiple Logistic Regression Analysis for Presence of Reflux Esophagitis

Factors	Odds ratio	95%CI	p value
Gender (male)	2.550	1.632-3.984	<0.001
Age (1-year increments)	1.006	0.990-1.002	0.454
BMI	1.130	1.084-1.178	<0.001
Presence of esophageal cardiac glands	0.324	0.162-0.646	0.001
Gastric mucosal atrophy*			
moderate	0.419	0.287-0.612	<0.001
severe	0.243	0.109-0.542	<0.001
Size of diaphragmatic hiatus**			
1-2 cm	1.758	1.320-2.341	<0.001
>2 cm	5.847	3.723-9.185	<0.001
Habitual drinking	1.082	0.817-1.433	0.583
Smoking habit	1.627	1.217-2.175	0.001

*Odds ratio calculated in comparison to subjects with mild atrophy.
**Odds ratio calculated in comparison to subjects with diaphragmatic hiatus sized 0-1 cm.

Table 3. Multiple Logistic Regression Analysis for Presence of GERD Symptoms

Factors	Odds ratio	95%CI	p value
Gender (male)	0.918	0.747-1.128	0.417
Age (1-year increments)	0.996	0.987-1.005	0.399
BMI	1.044	1.016-1.073	0.021
Presence of esophageal cardiac glands	0.909	0.706-1.170	0.459
Gastric mucosal atrophy*			
moderate	1.199	0.988-1.455	0.067
severe	0.655	0.459-0.935	0.020
Size of diaphragmatic hiatus**			
1-2 cm	1.256	1.057-1.493	0.010
>2 cm	1.990	1.345-2.944	<0.001
Habitual drinking	0.995	0.831-1.190	0.952
Smoking habit	1.317	1.077-1.611	0.007

*Odds ratio calculated in comparison to subjects with mild atrophy.
**Odds ratio calculated in comparison to subjects with diaphragmatic hiatus sized 0-1 cm.

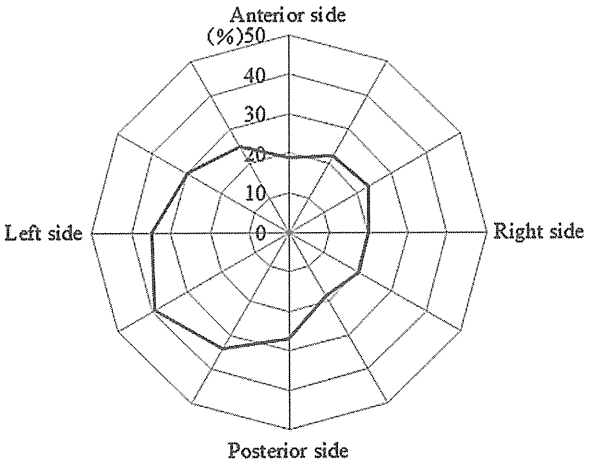

Figure 2. Circumferential localization of the esophageal cardiac glands in the 355 cases. The values represent the percentage of lesions on each side of the esophageal wall.

Discussion

Esophageal cardiac glands are found in the proper mucosal layer of the distal end of the esophagus, although their origin has not been determined (8). These lesions have been reported to be more frequently observed endoscopically in patients with *H. pylori* infection than in those without, and it has been suggested that *H. pylori* infection-induced carditis stimulates hypertrophic changes in esophageal cardiac glands (9). The present results also showed that individuals possessing visible esophageal cardiac glands have more severe gastric mucosal atrophy, which is primarily caused by long-term *H. pylori* infection in Japanese individuals. Therefore, *H. pylori* infection is considered to correlate with the presence of endoscopically visible esophageal cardiac glands, although the mechanisms underlying the hypertrophic changes observed in esophageal cardiac glands can-

magnifying endoscopic study of esophageal cardiac gland: what role does esophageal cardiac gland play at the esophago-cardiac junction? Dig Endosc **17** (Supple): S11-S16, 2005.

10. Yagi K, Nakamura A, Sekine A, Umezu H. The prevalence of esophageal cardiac glands: relationship with erosive esophagitis and nonerosive reflux disease (NERD) in Japanese patients. Endoscopy **38**: 652-653, 2006.
11. Carlsson R, Dent J, Bolling-Sternevald E, et al. The usefulness of a structured questionnaire in the assessment of symptomatic gastroesophageal reflux disease. Scand J Gastroenterol **33**: 1023-1029, 1998.
12. Lundell LR, Dent J, Bennett JR, et al. Endoscopic assessment of oesophagitis: clinical and functional correlates and further validation of the Los Angeles classification. Gut **45**: 172-180, 1999.
13. Kimura K, Takemoto T. An endoscopic recognition of the atrophic border and its significance in chronic gastritis. Endoscopy **3**: 87-97, 1969.
14. Miki K, Ichinose M, Shimazu A. Serum pepsinogen as a screening test of extensive chronic gastritis. Gastroenterol Jpn **22**: 133-141, 1987.
15. Azumi T, Adachi K, Arima N, et al. Five-year follow-up study of patients with reflux symptoms and reflux esophagitis in annual medical check-up field. Intern Med **47**: 691-696, 2008.
16. Chiba H, Gunji T, Sato H, et al. A cross-sectional study on the risk factors for erosive esophagitis in young adults. Intern Med **51**: 1293-1299, 2012.
17. Higuchi K, Joh T, Nakada K, Haruma K. Is proton pump inhibitor therapy for reflux esophagitis sufficient?: a large real-world survey of Japanese patients. Intern Med **52**: 1447-1454, 2013.
18. Fass R, Fennerty MB, Vakil N. Nonerosive reflux disease: current concepts and dilemmas. Am J Gastroenterol **96**: 303-314, 2001.
19. Rodriguez-Stanley S, Robinson M, Earnest DL, Greenwood-Van Meerveld B, Miner PB Jr. Esophageal hypersensitivity may be a major cause of heartburn. Am J Gastroenterol **94**: 628-631, 1999.
20. Nagahara A, Miwa H, Minoo T, et al. Increased esophageal sensitivity to acid and saline in patients with nonerosive gastroesophageal reflux disease. J Clin Gastroenterol **40**: 891-895, 2006.
21. Miwa H, Minoo T, Hojo M, et al. Oesophageal hypersensitivity in Japanese patients with non-erosive gastro-oesophageal reflux diseases. Aliment Pharmacol Ther **20**: 112-117, 2004.
22. Balaban DH, Yamamoto Y, Liu J, et al. Sustained esophageal contraction: a marker of esophageal chest pain identified by intraluminal ultrasonography. Gastroenterology **116**: 29-37, 1999.
23. Pehlivanov N, Liu J, Mittal RK. Sustained esophageal contraction: a motor correlate of heartburn symptom. Am J Physiol Gastrointest Liver Physiol **281**: G743-G751, 2001.
24. Wiklund I, Carlsson R, Carlsson J, Glise H. Psychological factors as a predictor of treatment response in patients with heartburn: a pooled analysis of clinical trials. Scand J Gastroenterol **41**: 288-293, 2006.
25. Katsube T, Adachi K, Furuta K, et al. Difference in localization of esophageal mucosal breaks among grades of esophagitis. J Gastroenterol Hepatol **21**: 1656-1659, 2006.
26. Kinoshita Y, Furuta K, Adachi K, Amano Y. Asymmetrical circumferential distribution of esophagogastric junctional lesions: anatomical and physiological considerations. J Gastroenterol **44**: 812-818, 2009.
27. Ohara S, Furuta K, Adachi K, et al. Radially asymmetric gastroesophageal acid reflux in the distal esophagus: examinations with novel pH sensor catheter equipped with 8 pH sensors. J Gastroenterol **47**: 1221-1227, 2012.
28. Satoh K, Kimura K, Yoshida Y, et al. Relationship between *Helicobacter pylori* and atrophic gastritis. Eur J Gastroenterol Hepatol **6**: S85-S88, 1994.
29. Koike T, Ohara S, Sekine H, et al. *Helicobacter pylori* infection inhibits reflux esophagitis by inducing atrophic gastritis. Am J Gastroenterol **94**: 3468-3472, 1999.
30. Kinoshita Y, Kawanami C, Kishi K, Nakata H, Seino Y, Chiba T. *Helicobacter pylori* independent chronological change in gastric acid secretion in the Japanese. Gut **41**: 452-458, 1997.
31. Shirota T, Kusano M, Kawamura O, et al. *Helicobacter pylori* infection correlates with severity of reflux esophagitis: with manometry findings. J Gastroenterol **34**: 553-559, 1999.
32. Fujishiro H, Adachi K, Kawamura A, et al. Influence of *Helicobacter pylori* infection on the prevalence of reflux esophagitis in Japanese patients. J Gastroenterol Hepatol **16**: 1217-1221, 2001.

J Gastroenterol
DOI 10.1007/s00535-014-1027-y

The Japanese Society of Gastroenterology

ORIGINAL ARTICLE—ALIMENTARY TRACT

No increase in gastric acid secretion in healthy Japanese over the past two decades

Norihisa Ishimura · Yasuko Owada · Masahito Aimi · Tadayuki Oshima · Tomoari Kamada · Kazuhiko Inoue · Hironobu Mikami · Toshihisa Takeuchi · Hiroto Miwa · Kazuhide Higuchi · Yoshikazu Kinoshita

Received: 12 September 2014 / Accepted: 2 December 2014

Abstract
Background The prevalence of gastroesophageal reflux disease (GERD) has been increasing worldwide over recent decades. A previous study demonstrated that gastric acid secretion, thought to be an important factor in the increase in the rate of GERD, in Japanese individuals increased in the era from the 1970s to the 1990s. The aim of this study was to evaluate whether gastric acid secretion has altered over the past two decades with and without the influence of *Helicobacter pylori* infection in nonelderly and elderly Japanese.
Methods Gastric acid secretion, the concentrations of serum gastrin, pepsinogen I, and pepsinogen II, and *H. pylori* infection were determined in 78 healthy Japanese subjects. The findings were compared with data obtained in the 1990s.
Results Basal acid output (BAO) and maximal acid output (MAO) gradually decreased with age in *H. pylori*-negative subjects. In addition, those with *H. pylori* infection tended to show decreased gastric acid secretion as compared with those without infection, particularly in the elderly group. MAO decreased gradually with age in males, whereas it remained unchanged with age in females. MAO in *H. pylori*-negative subjects has not changed over the past two decades (17.7 mEq/h vs 17.6 mEq/h in nonelderly subjects, and 15.2 mEq/h vs 12.7 mEq/h in elderly subjects).
Conclusions In contrast to the increased prevalence of GERD, gastric acid secretion has not increased over the past two decades in Japanese. However, secretion has decreased with age in males but not in females, which may partly explain the sex difference in the age-related GERD prevalence.

Keywords Basal acid output · Maximal acid output · Gastrin · *Helicobacter pylori*

Abbreviations

BAO	Basal acid output
BMI	Body mass index
GERD	Gastroesophageal reflux disease
MAO	Maximal acid output

Introduction

The prevalence of gastroesophageal reflux disease (GERD) varies throughout the world [1], as epidemiology studies have reported a prevalence ranging from 10 to 20 % in

N. Ishimura (✉) · M. Aimi · H. Mikami · Y. Kinoshita
Department of Gastroenterology and Hepatology, Shimane University School of Medicine, 89-1 Enya-cho, Izumo, Shimane 693-8501, Japan
e-mail: ishimura@med.shimane-u.ac.jp

Y. Owada
Osaka Pharmacology Clinical Research Hospital, Osaka, Japan

T. Oshima · H. Miwa
Division of Gastroenterology, Department of Internal Medicine, Hyogo College of Medicine, Nishinomiya, Japan

T. Kamada
Division of Gastroenterology, Department of Internal Medicine, Kawasaki Medical School, Kurashiki, Japan

K. Inoue
Department of General Medicine, Kawasaki Medical School, Kurashiki, Japan

T. Takeuchi · K. Higuchi
Second Department of Internal Medicine, Osaka Medical College, Takatsuki, Japan

Published online: 14 December 2014

Western countries and lower rates in Asia [2, 3]. The reasons remain obscure, although genetic differences, differences in *Helicobacter pylori* prevalence, and lifestyle factors such as obesity may have an influence [4–6]. In recent decades, GERD has become more prevalent in Asia, including Japan [7–9], which is thought to be due to several factors, including the Westernization of eating habits, a decrease in the *H. pylori* infection rate, increased gastric acid secretion, an increase in the number of aged individuals, and more attention being paid to the disease [10–12].

Gastric acid secretion is affected by various factors, including race, sex, and age [13]. Studies conducted in the 1990s showed that gastric acid secretion in Japanese subjects increased from the 1970s to the 1990s, although it remained lower than that in Europeans and North Americans [14–16]. However, along with changes in the social environment to a more Western one over the past two decades in Japan, it has not been elucidated whether that increasing trend has continued from the 1990s to the present. The increasing prevalence of GERD in Japan has led to speculation that the rate may rise continuously. In this study, we sought to determine the effects of age and sex on gastric acid secretion in healthy asymptomatic Japanese subjects, and also evaluated whether gastric acid secretion has changed over the past two decades with and without the influence of *H. pylori* infection in nonelderly and elderly Japanese.

Methods

Participants

Healthy adult Japanese volunteers residing in the Kansai area who consented to participate in the study were screened precisely using the specific medical record to evaluate the present illness, past and medication history, and the blood test. Then, enrolled subjects were divided into those aged between 20 and 25 years (young group), around 50 years (nonelderly), and around 75 years (elderly). Exclusion criteria were a history of gastrointestinal diseases, including GERD, peptic ulcer, functional dyspepsia, gastric surgery, malignancy, treatment for *H. pylori* eradication, or renal failure. Individuals who had gastrointestinal symptoms and those taking medications known to affect gastric acid secretion were also excluded. *H. pylori* infection was diagnosed by positive results of both the urea breath test (UBIT tablets/UBiT-IR300, Otsuka Pharmaceutical, Tokyo, Japan/Otsuka Electronics, Osaka, Japan) and the serum antibody test (E-plate EIKEN *H. pylori* IgG antibody II, Eiken Chemical, Tokyo, Japan). Eligible volunteers were assigned to one of the following five groups: elderly with *H. pylori* infection, elderly without *H. pylori* infection, nonelderly with *H. pylori* infection, nonelderly without *H. pylori* infection, and young without *H. pylori* infection (Fig. 1). The study protocol was designed to include nearly equal numbers of males and females within each group of 15, for a total of 75 subjects. The sample size of the subjects in each group was estimated to adjust the findings of the previous study [16], because a major aim of the study was to compare current with previous data obtained in the 1990s. This study was conducted at a single center between October 2012 and October 2013. Prior approval was received from the Institutional Review Board of Osaka Pharmacology Clinical Research Hospital, and the study was conducted in accordance with the Declaration of Helsinki. All subjects provided written informed consent prior to participation. This study is registered with the University Hospital Medical Information Network (UMIN) clinical trials registry (UMIN000008906). All authors had access to the clinical data and approved the final version of the manuscript.

Measurement of gastric acid secretion

Gastric acid secretion was measured in the same manner as in our previous study reported in 1997 [16]. Measurements started at around 8:00 A.M. after a 12-h fast. A large (4.0-mm) nasogastric tube with multiple openings (Salem Sump dual-lumen stomach tube, Covidien) was inserted into the stomach, and gastric juice was aspirated. In some cases, an X-ray examination was used to determine whether the tube was correctly positioned in the stomach. After residual gastric contents had been removed by aspiration, basal acid output (BAO) was

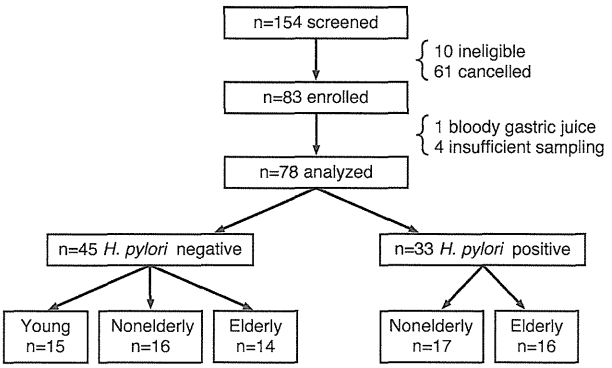

Fig. 1 Flow diagram of enrolled subjects. Screening assessments of 154 healthy adult Japanese volunteers aged between 20 and 25 years (young group), around 50 years (nonelderly), and around 75 years (elderly) were conducted. Eligible volunteers ($n = 78$) were assigned to the following groups: elderly with *Helicobacter pylori* infection ($n = 16$), elderly without *H. pylori* infection ($n = 14$), nonelderly with *H. pylori* infection ($n = 17$), or nonelderly without *H. pylori* infection ($n = 16$), and young without *H. pylori* infection ($n = 15$)

measured by titrating the acidity of the gastric juice collected for 1 h as a sum of six 10-min outputs. Maximal acid output (MAO) was then measured by administrating pentagastrin (Alliance Pharmaceuticals, Chippenham, UK/AnazaoHealth, Tampa, FL, USA) intramuscularly at 6 μg per kilogram of body weight and collecting the gastric juice for an additional hour as the sum of six 10-min outputs after pentagastrin injection. Gastric juice was collected with the subject in a supine or left lateral recumbent position to allow for complete aspiration. Samples were titrated to pH 7.0 with NaOH, and all results are expressed as milliequivalents (mEq) of acid per hour.

Assays of serum gastrin, pepsinogen I, and pepsinogen II

Serum gastrin, pepsinogen I, and pepsinogen II were measured using blood samples obtained early in the morning on the same day as the BAO/MAO measurements. Serum was separated and stored at −80 °C until the assays. The serum gastrin concentration was measured by radioimmunoassay (Gastrin Riakit II, TFB, Tokyo, Japan), whereas the concentrations of pepsinogen I and pepsinogen II were measured by a latex agglutination test (Lasay Autopepsinogen I/II, SHIMA Laboratories, Tokyo, Japan).

Statistical analysis

The values for BAO, MAO, serum gastrin, serum pepsinogen I, pepsinogen II, and the ratio of pepsinogen I to pepsinogen II were compared among the three groups without *H. pylori* infection, between the two groups with *H. pylori* infection, and between *H. pylori*-positive and *H. pylori*-negative subjects divided by age. Comparisons between groups were performed using the Mann–Whitney *U* test. Changes in MAO and serum gastrin concentration from those determined in the 1970s and 1990s [16], the primary end point of this study, were analyzed with the Kruskal–Wallis test. Post hoc analysis using the Mann–Whitney *U* test with Bonferroni correction was performed when the Kruskal–Wallis test result was determined to show a significant difference. Sex differences in relation to age, body weight, body height, and body mass index (BMI) with regard to BAO and MAO were analyzed by single regression analysis. Regression coefficients of age, body weight, body height, and BMI were compared between the sexes using Student's *t* test. All statistical tests were performed in a two-sided manner and a *p* value of less than 0.05 (less than 0.025 under Bonferroni correction) was considered to indicate significance. All statistical analyses were performed using JMP 9.0 (SAS Institute, Cary, NC, USA).

Results

Characteristics of subjects

A flow diagram of the enrolled subjects is shown in Fig. 1. Of 83 enrolled subjects, five were excluded from the analysis because of bloody gastric juice ($n = 1$), or insufficient sampling ($n = 4$). The characteristics of the *H. pylori*-positive and *H. pylori*-negative subjects after they have been divided by age (young, nonelderly, elderly) are shown in Table 1. The mean age of the young *H. pylori*-negative group was 22.9 ± 1.9 years (mean ± standard deviation) years. The age and sex distribution was not different among the groups with or without *H. pylori* infection. The groups did not differ in regard to mean height, mean body weight, and mean BMI.

Changes in gastric acid secretion by age and *H. pylori* infection

First, we evaluated gastric acid secretion in each group by age (Table 1, Fig. 2). In the *H. pylori*-negative groups, BAO gradually decreased with age, and that decrease was significantly different between the young and nonelderly groups, and the young and elderly groups ($p < 0.01$ and $p < 0.01$, respectively; Fig. 2a). Among nonelderly subjects, BAO was lower in the *H. pylori*-positive group than in the *H. pylori*-negative group, although it was not significant. In contrast, BAO was significantly lower in the elderly subjects who were *H. pylori* positive ($p < 0.01$).

MAO was associated with age and *H. pylori* infection in the same manner as BAO (Fig. 2b). In *H. pylori*-negative subjects, MAO was significantly lower in the elderly group than the nonelderly group ($p < 0.05$). In elderly subjects, MAO was significantly lower in the *H. pylori*-positive subjects than in the *H. pylori*-negative subjects ($p < 0.05$).

Gastrin is the main stimulant of gastric acid secretion. Serum gastrin concentration was significantly higher in the elderly subjects as compared with nonelderly subjects who were *H. pylori* negative ($p < 0.05$), suggesting that it was stimulated by lower gastric acid secretion as a feedback stimulation (Fig. 2c). Both elderly and nonelderly *H. pylori*-positive subjects had higher serum gastrin concentrations than their respective *H. pylori*-negative counterparts ($p < 0.05$ and $p < 0.01$, respectively), which was consistent with evidence that *H. pylori* infection causes gastric atrophy and thereby induces hypergastrinemia [17, 18].

A significant correlation between serum pepsinogen values and gastric acid secretion has been reported in many previous reports [19]. In the nonelderly group, the pepsinogen I to pepsinogen II ratio was consistently lower for all ages of *H. pylori*-positive subjects as compared with